

PEOPLE'S DEMOCRATIC REPUBLIC OF ALGERIA
MINISTRY OF HIGHER EDUCATION AND SCIENTIFIC RESEARCH



UNIVERSITY BLIDA 1
FACULTY OF TECHNOLOGY
DEPARTMENT OF MECHANIC
RESEARCH LABORATORY OF STRUCTURE « L.S »

Project Graduation

For Obtaining the Master's Degree In

Mechanical Construction

**Dynamic Behavior of a Manipulator Robot Excited
by an External Force/ Application to Rivet Assembly**

Realized by:
BOUABACHE Nour Elhouda
BOUCHAMI Hiba

Proposed and supervised by:
Professor Mohammed OUALI
Mr. OSMANI El Hadi

2021/2022

Appreciation

*We would like to start by thanking **Allah Almighty** for giving us the strength, the courage and the patience to complete this thesis .*

We would like to thank Professor Mohammed OUALI , MR. OSMANI El Hadi and Mr Lounici Bilel as well ,for their guidance and supervision through out our months of work , a work that would not have been accomplished without their help , we are really grateful and thankful to the experience .

We are so thankful to everyone who helped us and supported us during all these years of study especially our teachers .

Dedication

We want to dedicate this work to our beautiful and loving families , to our supporting friends , to our great teachers Mr.Ouali , Mr.OSMANI El Hadi and Mr.LOUNICI Bilel , to everyone who ever supported us and believed in us .

Thank you all so much

Hiba and Nour El Houda

Abstract

In this work, we propose to study the installation of aluminum rivets, applying force to the rivet to assemble parts, this operation will be carried out by a robot (Staubli TX90) with four rotoid joints, the robot is equipped with a pneumatic hammer that will generate a series of shocks to deform the cylindrical head of the rivet. The latter will take on a permanent domed shape. This operation will excite the structure which will in turn be susceptible to vibrations. To carry out this work, we blocked the joint 4 and 6, and we modeled the structure using SolidWorks in different configurations to calculate the natural frequencies in order to avoid the resonance of the robot structure, then, we studied the inverse dynamics of the robot to verify its operation under the effect of the weight of the tool which is the pneumatic hammer.

ملخص:

ي هذا العمل، نقترح دراسة تركيب المسامير المصنوعة من الألومنيوم، بتطبيق القوة على البرشام لتجميع الأجزاء، وسيتم تنفيذ هذه العملية بواسطة روبوت (Staubli TX90) بأربعة مفاصل دوارة، وقد تم تجهيز الروبوت بمطرقة هوائية ستولد سلسلة من الصدمات لتسوية رأس البرشام الأسطواني. هذا الأخير سيأخذ شكل قبة دائمة. ستثير هذه العملية الهيكل الذي سيكون بدوره عرضة للاهتزازات. لتنفيذ هذا العمل، قمنا بحظر المفصل 4 و 6، وقمنا بتصميم الهيكل باستخدام SolidWorks في تكوينات مختلفة لحساب الترددات الطبيعية من أجل تجنب صدى بنية الروبوت، ثم درسنا الديناميات العكسية للروبوت للتحقق من تشغيله تحت تأثير وزن الأداة وهي المطرقة الهوائية.

Résumé

Dans ce travail, nous proposons d'étudier la mise en place de rivets en aluminium, en appliquant une force sur le rivet pour assembler des pièces, cette opération sera réalisée par un robot (Staubli TX90) à quatre articulations rotoïdes, le robot est équipé d'un marteau pneumatique qui va générer une série de choc pour déformer la tête cylindrique du rivet. Ce dernier va prendre une forme bombée permanente. Cette opération va exciter la structure qui va être à son tour susceptible a des vibrations. Pour réaliser ce travail, on a bloqué l'articulation 4 et 6, et on a modélisé la structure en utilisant solidworks sous différentes configurations pour calculer les fréquences propres dans le but d'éviter la résonance de la structure du robot, ensuite, nous avons étudié la dynamique inverse du robot pour vérifier son fonctionnement sous l'effet du poids de l'outil qui est la marteau pneumatique.

List of figures

Figure I.2 : Humanoid robot (ASIMO)

Figure I.3 : Mobile robot

Figure I.4 : Industrial robot

Figure I.5 : Manipulator arm

Figure I.6 : Prismatic joint

Figure I.7 : Rotoid joint

Figure I.8 : The sensors

Figure I.9 : Cartesian robot

Figure I.10 : Cylindrical robot

Figure I.11 : Spherical robot

Figure I.12 : 3R robot.

Figure I.13 : SCARA robot.

Figure I.14 : Riveting process

Figure I.15 : Rivets on an airplane

Figure I.16 : Types of rivets

Figure II.1 : rivet

Figure II.2 : deformation of the head of the rivet

Figure II.3 : ROBOT Staubli RX90 six axes

Figure II.4 : “Geometric” zero configuration

Figure II.5 : Geometric parameters in the case of a simple open structure

Figure II.6 : Geometric dimensions of the StäubliX-90 robot

Figure II.7 : 8 solutions possibles for IGM of TX 90

Figure II.8 : Assessment of forces, speeds and accelerations

Figure II.9 : Forces and moments on link

Figure III.1: Parts assembled by the cold-deformed rivet

Figure III.2 : A choc modeled by a half sinusoid

Figure III.3: Making a joint by rivet manually

Figure III.4: Acceleration measurement of a pneumatic hammer during the installation of a rivet.

Figure IV.1: Deformable toe rivet

Figure IV.2: The cylinder

Figure IV.3: The Piston

Figure IV.4: The spring

Figure IV.5: Riveting tool

Figure IV.6 Riveting tool and tool flange

Figure IV.7: Joint positions for Riveting Configuration n°4

Figure IV.8: Joint velocities for Riveting Configuration n°4

Figure IV.9: joint accelerations for Riveting Configuration n°4

Figure IV.10 : Joint torques for Riveting Configuration n°4

Figure IV.11 : 1st configuration of the riveting

Figure IV.12 : Modal distortion and natural frequencies of the 1st configuration

Figure IV.13 : 2nd configuration of the riveting

Figure IV.14 : Modal distortion and natural frequencies of the 2nd configuration

Figure IV.15 : 3rd configuration of the riveting

Figure IV.16 : Modal distortion and natural frequencies of the 3rd configuration

Figure IV.17 : 4th configuration of the riveting

Figure IV.18 : Modal distortion and natural frequencies of the 4th configuration

List of tables

Table I.1 : Number of possible morphologies depending on the number of degrees of freedom of the robot.

Table II.1 : Denavit-Hartenberg (D-H) parameters of the StäubliX-90.

Table II.2 : TX-90 Rotation deflections.

Nomenclature

α_j : The angle between -1 and corresponding to rotation around X_{j-1} Rot ($X,$) [rad]

d_j : The distance between Z_{j-1} and Z_j along -1 , Trans ($X,$ d) [m]

θ_j : The angle between the axes -1 and corresponding to rotation around, Rot ($Z,$) [rad]

r_j : The distance between X_{j-1} and X_j along, Trans ($Z,$ r) [m]

$q_j = \theta_j$: Vector of joint variables [rad]

${}^j{}^{-1}\mathbf{T}$: The homogeneous transformation matrix

${}^j{}^{-1}\mathbf{P}_j$: Position vector [m]

${}^j{}^{-1}\mathbf{A}_j$: Orientation matrix [rad]

$\mathbf{J}(\mathbf{q})$: Jacobian matrix

Γ : Vector of torques/forces of actuators [N.m]

$\dot{\mathbf{q}}$: Vector of joint velocities [rad/s]

$\ddot{\mathbf{q}}$: Vector of joint accelerations [rad/s²]

$\dot{\mathbf{X}}$: Speed of operational variables [m/s]

$\ddot{\mathbf{X}}$: Cartesian acceleration [m/s²]

\mathbf{I}_{aj} : Moments of inertia of actuators [N.m/rad/s²]

\mathbf{V}_n : Translation speed [m/s]

ω_n : Rotation speed [rad/s]

\mathbf{a}_j : unit vector

\mathbf{M}_j : Body mass [kg]

${}_j\mathbf{V}$: Linear velocity vector [m/s]

${}_j\boldsymbol{\omega}$: Angular velocity vector [rad/s]

Γf : Couple of friction [N.m]

\mathbf{F}_s : Dry friction [N.m]

Fv_j : Viscous friction [N.m/rad/s]

ω : Frequency of the hammer

\mathbf{M} : The mobile mass of the hammer

Table of Contents

Appreciation.....	II
Dedication.....	III
Abstract:.....	IV
List of figures.....	V
List of Tables	VII
Nomenclature	VIII
State of the art.....	1

Chapter I: Introduction to Robotics

I.1. Definition of a robot	2
I.2. Types of robots	3
A. Humanoids	3
B. Mobile robots	3
C. Industrial robots.....	4
I.3. Definition of a manipulator arm.....	4
I.4.The components of a manipulator arm.....	5
A. The joints.....	5
1. Prismatic joints.....	5
2. The rotoid joints.....	6
B. The sensors.....	6
C. The command.....	7
I.5.The workspace.....	7
A. Joint space.....	7
B. The operational space.....	7

I.6. The different types of manipulator robots that exist on the market.....	7
A. Cartesian structure (PPP).....	7
B. Cylindrical structure (RPP or PRP).....	8
C. The spherical structure (RRT or RRP).....	8
D. The anthropomorphic structure (RRR).....	9
E. The SCARA structure.....	9
I.7. Morphologies of robot-manipulators.....	9
I.8. Redundancy.....	10
I.9. Singular configuration.....	10
I.10. Rivet assembly.....	11
I.11 .Classification of rivets.....	13
Conclusion.....	13

Chapitre II: Modelisation of the robot

II.1 Introduction:	14
II.2 Choice of the robot and its associated models.....	15
II.3 Geometric model.....	16
A. Denavit-Hartenberg settings.....	16
B. Transformation matrix.....	19
II.3.1 Direct geometric model (DGM).....	19
II.3.2 Inverse Geometric Model (IGM).....	21
II.4 kinematic model.....	25
II.4.1 Methods for calculating the Jacobian matrix.....	26
II.4.2 First Order Inverse Kinematic Model.....	28
II.4.3 Second Order Inverse Kinematic Model.....	28
II.5 The dynamic model.....	28
II.5.1 Inverse dynamic model (IDM).....	29

The Newton Euler's formalism.....	29
Algorithme for calculating actuator forces (NE).....	34
Conclusion.....	35

Chapter III. Natural frequencies ,eignmodes

III.1 Introduction:.....	36
III.2 Resonance.....	36
III.3 Method for calculating frequencies and eigenmodes.....	37
II.4 Modeling the force generated by the pneumatic hammer.....	38
A) Half sinusoid model.....	39
B) A series of Dirac impulses.....	39
C) The unbalance.....	39

Chapter IV : Riveting application

IV.1 Introduction.....	41
IV.2 The rivet.....	41
IV.3 Riveting tool.....	42
IV.4 Inverse dynamics of the system in a free trajectory.....	48
Commantary.....	52
IV.2 Vibration study using Solidworks software.....	52
Commantary.....	59
Conclusion.....	60
General conclusion.....	61
References	62
Appendix A.....	64
Appendix B.....	73

State of the art

Currently robots replace the work of man in several fields ranging from the generation of a simple trajectory by a robot such as paint stains, welding to the realization of very difficult tasks such as surgical operations in medicine, the manufacture of microchips, etc. artificial intelligence aims to improve their performance. This performance race generates complex systems whose risks of malfunction is very probable and can jeopardize the system and its environment among the causes of malfunctioning vibrations. The phenomenon of vibration of the manipulator during operation, affects the accuracy of the trajectory and the stability of the dynamics of the manipulator and may even lead to damage to the actuators of the robot and its structure. Consequently, the simulation of these systems is damaged, a great necessity for predicting the risks of malfunctioning. The causes of vibration are generally explored, then solutions are proposed according to the potential causes [1]. However, there are many factors that can cause the vibration of the mechanical arm, such as the resonance of the mechanical arm, insufficient rigidity of the transmission gears, the output torque of the motor does not match the actual demand, low precision installation and transmission clearance, the non-linear friction of the arm joint, often these influencing factors are coupled, which increases the degree of complexity of vibrations. Several works have been published in this field such as the reduction of vibrations of the manipulator arm [1] the author modeled the robot manipulator by a double pendulum, [2] uses a more complicated model where it takes into consideration the longitudinal vibrations of the bodies that make up the manipulator [3] models the connection between the robot and its environment by a system composed of two springs and two shock absorbers in two directions. In this work, it is proposed to study the placement of an aluminum rivet, by applying a force on the rivet to assemble parts, this operation will be carried out by a robot with four rotary joints, the robot is equipped with a pneumatic hammer that will generate a series of impacts to deform the cylindrical head of the rivet. The latter will take on a permanent domed shape. This operation will excite the structure which will in turn be susceptible to vibrations.

Chapter I: Introduction to Robotics

Robots generally consist of three subsystems: a subsystem for generating motion (mechanical structure), a subsystem for perceiving sensors and cameras, and an automaton computer control subsystem (Fig I.1).

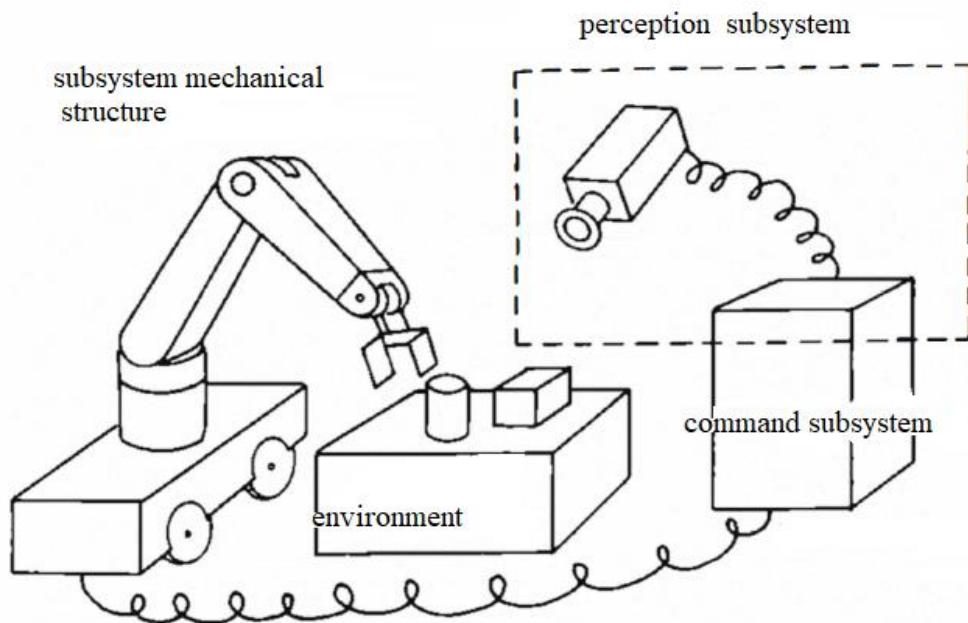


Figure I.1 The subsystems of a manipulator arm

Today, robots are tools Necessary in a manufacturing environment, Robots are taking hold as technology advances More and more in modern industry. Currently, researchers are able to design lightweight and fast robots. [4]

These machines are increasingly used in industry and research, which makes it possible to handle with great precision, and therefore in a safer way, various products or objects, neutral or dangerous.

I.1. Definition of a robot:

A robot is an object that possesses three properties:

- It is a physical object.
- It functions autonomously.

- It is functioning in a situated manner.

This means a robot is a programmed physical entity that perceives and acts autonomously within a physical environment which has an influence on its behaviour. In addition, the robot is situated, it manipulates not only information but also physical things.

In addition, the International Federation of Robotics (IFR) distinguishes two main services provided by robots: (a) in the service of humans (personal protection, entertainment, etc.) and (b) maintenance equipment (maintenance, repair, cleaning etc.) and focus on a task. [5]

I.2. Types of robots:

A. Humanoids:

Largely thanks to science fiction this is the most well-known category, it includes all anthropomorphic robots whose form is reminiscent of human morphology (Fig. 1.2).



Figure I.2 Humanoid robot (ASIMO)

B. Mobile robots:



Figure I.3 Mobile robot

This category encompasses all robots with a mobile base, but generally refers to the subcategory of mobile robots with wheels; other robots are generally referred to by their category names matching their functionality as it is attached in (Fig 1.3).

C. Industrial robots:



Figure I.4 Industrial robot

The majority of these robots are fixed-base. When the base is not fixed, it is usually mounted to a rail. We find in this category manipulator robots as shown in (Fig 1.4). [6]

I.3. Definition of a manipulator arm:

Today the most useful and efficient robotic systems are the industrial robot manipulators which can replace the human workers in difficult or monotonous jobs, or where a human would otherwise be faced with hazardous conditions. The robot manipulator consists of a robot arm, wrist, and gripper (Fig. 1.5). The robot arm is a serial chain of three rigid segments, which are relatively long and provide positioning of the gripper in the workspace. Neighboring segments of a robot arm are connected through a robot joint, which is either translational (prismatic) or rotational (revolute). The rotational joint has the form of a hinge and limits the motion of two neighbor segments to rotation around the joint axis. [7]

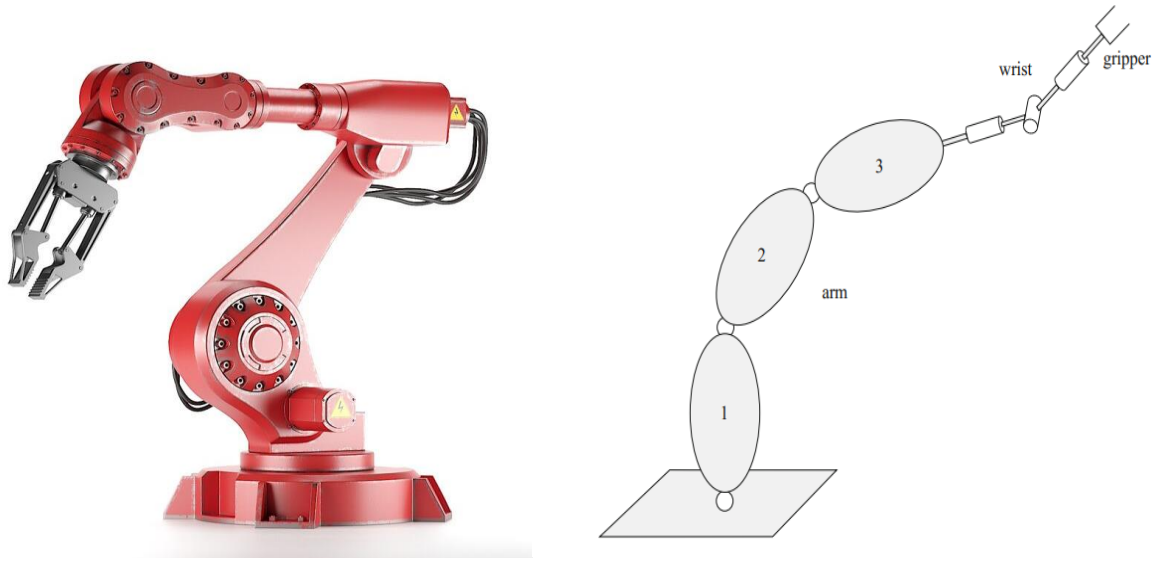


Figure I.5 Manipulator arm

Robotics has become an engineering field that uses computer science to design, manufacture, operate, and use robots. It is a multidisciplinary field that uses mechanics, electronics, computer science and information engineering. Robotics can be divided into five main areas: sensors, softs, mobility, human-machine interface and manipulation. It has also been divided into four major divisions: organic, industrial, mobile and air. [8]

I.4.The components of a manipulator arm:

A. The joints:

An articulation binds two successive bodies by limiting the number of degrees of freedom of one relative to the other. A complex joint can be reduced to a combination of prismatic or rotoid joints.

1. Prismatic joints :



Figure I.6 Prismatic joint

This is a slide-type joint, noted P, reducing the movement between two bodies to a translation along a common axis. The relative situation between the two bodies is measured by the distance along this axis (Fig. I.6).

2. The rotoid joints:

This is a pivot-type joint, noted R, reducing the movement between two bodies to a rotation about an axis common to them. The relative position between the two bodies is given by the angle about this axis (Fig. I.6).



Figure I.7 Rotoid joint

B. The sensors:

Sensors are elements whose purpose is to provide information about the system state. In robotics, two types of sensors are distinguished:

- Proprioceptive sensors:

This type of sensor is intended to give the real quantities of the position, speed and acceleration of the torque developed at each joint, in order to ensure, by servo control, the correct tracking of imposed trajectories.

- Exteroceptive sensors:

The objective is to collect information about the environment in order to perform the requested task (presence detection, contact, distance measurement, artificial vision). Depending on the planned task and the environment, the nature and amount of information to be collected vary widely. [9]



Figure I.8 The sensors

C. The command:

The control part synthesizes the instructions of the servos controlling the actuators, based on the perception function and the user's commands. It consists of:

- The human-machine interface through which the user programs the tasks that the robot must execute.
- The workstation or the environment in which the robot operates. [10]

I.5.The workspace:

A. Joint space:

The joints between the different bodies of a manipulator can be rotoid or prismatic. The joint space EA^n is therefore the Cartesian product of two types of spaces: \mathcal{R} for prismatic and the circle S^1 for rotoids. Let us cite the example of a manipulator with 6 dof with a cylindrical carrier and a ball joint, its morphology is written RPPRRR

and its articular space is written : $EA^n = EA^6 = S^1 \times \mathcal{R}^2 \times S^3$

B. The operational space:

The operational space EO^m describes the position and the orientation of the effector of a manipulator with n dof. The shape of this operational space depends on the parameters of the manipulator. For example, in the case of non-redundant manipulators with 3 dof , the operational space is therefore the Cartesian space of dimension 3: $EO^m = EO^3 = \mathcal{R}^3$.

As of the 6 dof manipulators, six position and orientation coordinates are used, thus we have: $EO^m = EO^6 = \mathcal{R}^3 \times SO(3)$.

Where $SO(3)$ represents the group of proper rotations of a rigid body in \mathcal{R}^3 . [11]

I.6. The different types of manipulator robots that exist on the market:

A. Cartesian structure (PPP):

This structure consists of three axes, which are driven by a translational movement. This particular type is less frequently used, except in a few specific applications such as gantry robots and shopping robots (Fig .I.9).

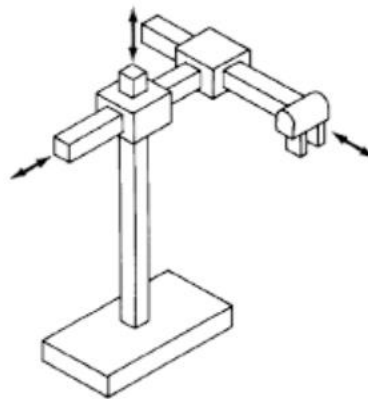


Figure I.9 Cartesian robot

B. Cylindrical structure (RPP or PRP):

This structure combines rotation and axial translation, supplemented by radial translation (Fig. I.10).

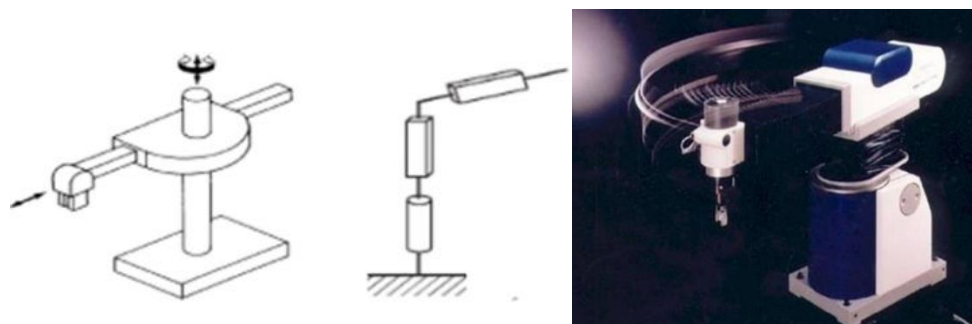


Figure I.10 Cylindrical robot

C. The spherical structure (RRT or RRP):

This structure associates two rotations (longitude and latitude) around orthogonal axes, supplemented by a radial translation (Fig. I.11).

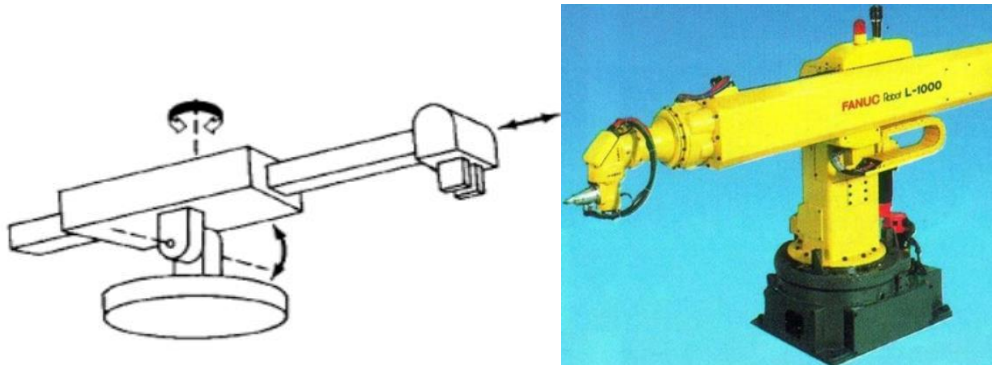


Figure I.11 Spherical robot

D. The anthropomorphic structure (RRR):

The wearer is in universal coordinates, also called poly-articulated configuration, three rotations, the last two of which are around parallel axes orthogonal to the first. The three joints corresponding respectively to the trunk (base), the shoulder and the elbow of a human being (Fig. I.12).

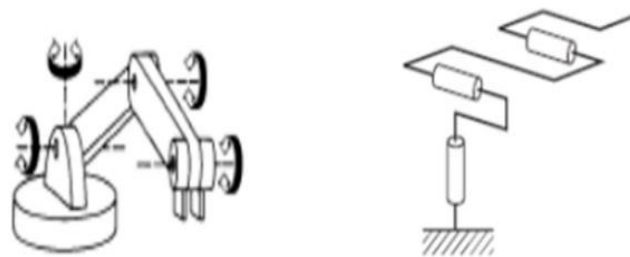


Figure I.12 3R robot.

E. The SCARA structure (Selective Compliance Arm for Robotic Assembly):

This architecture includes two rotations around two parallel axes, preceded or followed by a translation in the same direction (possibly this can be transferred to the wrist, which can also rotate around the same axis, i.e. a total of 4 ddm) . This structure is used in assembly operations (Fig. I.13). [12]

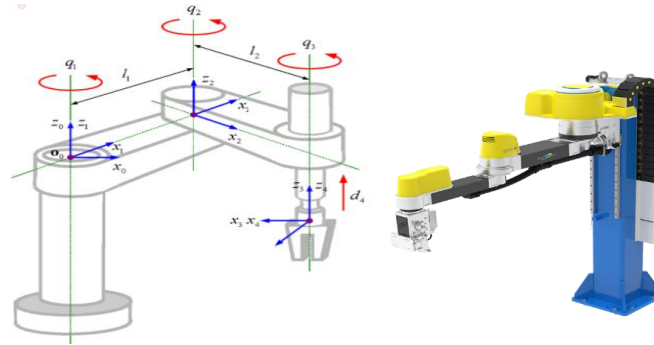


Figure I.13 SCARA robot.

I.7. Morphologies of robot-manipulators:

In order to enumerate the different possible architectures, only two parameters are considered: the type of joint (rotoidal or prismatic) and the angle between two successive articular axes (0 or 90). Generally, except in very special cases (last joints of the GMF PI50 or Kuka IR600 robots in particular); the consecutive axes are either parallel or perpendicular. The number of possible morphologies according to the number of joints is then deduced from the combination of the four values that these parameters can take (Table I.1).

Number of degrees of freedom of the robot	Number of structures
2	8
3	36
4	168
5	776
6	3508

Table I.1 Number of possible morphologies depending on the number of degrees of freedom of the robot.

It is conventionally agreed upon to call the first three degrees of freedom the carrier of the robot. The residual degrees of freedom form the wrist, characterized by much smaller dimensions and lower mass.

Considering these remarks, and based on the data in Table I.1, there are 36 possible wearer morphologies. Among these architectures, only 12 are mathematically different and non-redundant (we eliminate a priori the structures limiting the movements of the wearer to linear or planar displacements; i.e. three prismatic connections with parallel axes, or three rotary connections with parallel axes).[13]

I.8. Redundancy:

It is a situation of which the number of dof of the terminal organ is lower than the number of motorized joints. Redundant systems have the ability to perform an operational task while performing one or more additional tasks and/or respecting one or more constraints; such as avoiding obstacles moving away from singularities and joint stops. However, the exploitation of redundancy complicates the search for a solution. [14]

I.9. Singular configuration:

For all robots, whether they are redundant or not, it may be that in certain what supposedly called "singular configurations", the number of degrees of freedom of the end device is less than the dimension of the operational space. This case arises, for example, when two axes of prismatic joints are found parallel; or two axes of rotoid joints are found confused. [13]

Robotics makes it possible to carry out repetitive, painful, dangerous and versatile tasks with precision and reliability, in any kind of environment, at high and continuous speeds. It allows the overcoming the labor shortage and promoting a high productivity concomitantly, and thus giving a strong human, technical and economic interest. Such characteristic allowed robots to perform different tasks in different fields, especially in the industrial field:

- The transformation of parts: molding, machining, drilling, grinding, material removal.
- Surface preparation: painting, coating, thermal/plasma spraying, shot-blasting.
- Assembly: riveting, screwing, welding, insertion, gluing.
- Handling: handling of parts, machine loading/unloading, positioning.
- The distribution.
- Palletization and packaging.
- Inspection and testing.
- Cleaning. [15]

One of the tasks that manipulator arms perform in the industrial field is riveting (assembly by rivet):

I.10. Rivet assembly:

Rivets are assembly devices, used to link several parts. These are rods of steel, aluminum, brass, copper, etc [16]. To make an assembly by riveting, the rivet used must have

a length greater than the sum of the thicknesses of the assembled parts. Thus, the diameter of the hole, made on these parts, is greater than the diameter of the rivet, to facilitate assembly.

The connection between two thin parts (sheets) is made by deforming the end of the rivet, forming the second head. This operation, called “rivure”, results in a double shoulder that fixes the parts to be assembled against each other (Fig I.14).

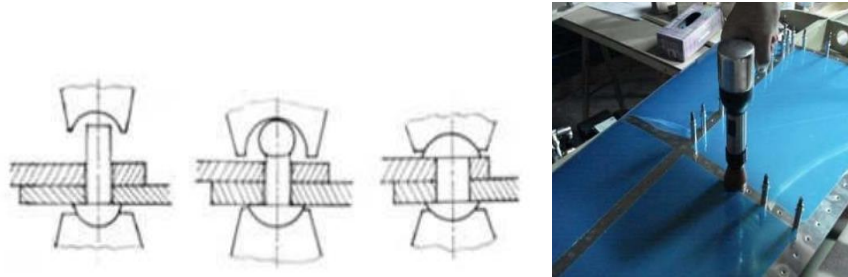


Figure I.14 Riveting process.

Steel rivets with a diameter of 10mm and more are set hot. While steel rivets with a diameter of less than 10mm, as well as light metal and copper rivets are cold fitted. [17]

Area of use for rivets:

The rivets constitute permanent assemblies. According to their destination, we traditionally distinguish:

- Strength rivets, which are encountered in metal constructions made of steel or light metals.
- Strength and sealing rivets, in boilermaking.
- Sealing rivets, in tanks, sheet metal chimneys, pipes without overpressure.
- The connecting rivets of sheet metal elements (aviation, automobile).

In many applications, rivets have been superseded by welding. A rivet requires more work, and welded parts are simpler and less expensive. In addition, the shaping of the button rivets puts the hearing of the workers to a tough test. However, the rivets are very safe and very easy to control (by sound, when hitting the assembly). Moreover, in the case of light alloys, we still often prefer the rivet, which makes it possible to avoid the consequences of the heating of welding.

Rivets are commonly used to join fuselage and wing sections of aircraft (Fig. I.15). Indeed, the assembly of an aircraft structure requires nearly 2,500,000 rivets, the installation of which

represents 30% of the total assembly time. Riveting is still widely used in applications where the lightness and strength demanded is critical, such as in an airplane . [18]



Figure I.15 Rivets on an airplane

I.11 .Classification of rivets:

Depending on the geometric shape, there are several types of rivet. (Fig I.16) represents the models most encountered in practice.[17]

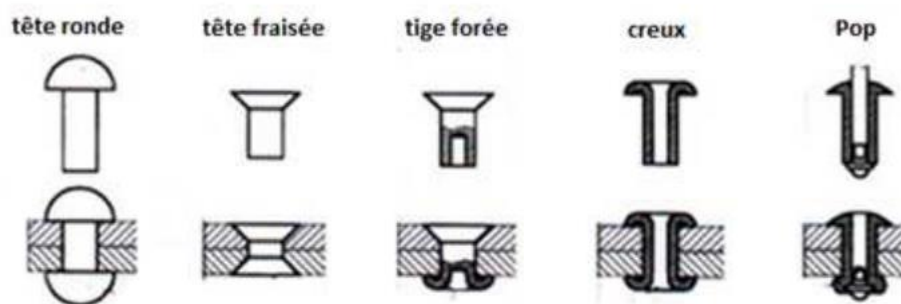


Figure I.16 Types of rivets

Conclusion :

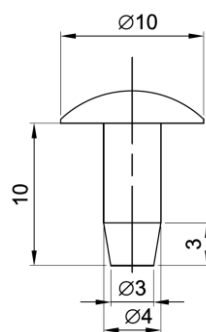
Today, machines are increasingly used in industry or research, especially the use of robots. This allows you to handle with much more precision and therefore in a safer way, various products or objects, neutral or dangerous.

In this first chapter, we have introduced the basics of robotics in general, which will be useful to us in the rest of our study.

Chapitre II :Modelisation of the robot

II.1 Introduction :

In this work, it is proposed to produce an assembly of two thin parts by riveting, the rivet used is made of aluminum 2017A with a cold-deformable head (FIG. 2.1). This task will be entrusted to a 4-axis manipulator robot, on its end effector is fixed a pneumatic hammer specially designed to deform the second head of the rivet, at the end, the rivet



FigureII.1 rivet

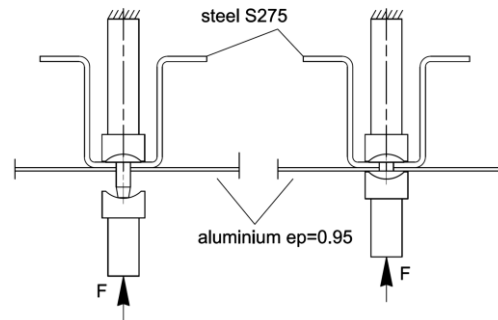


Figure II.2 deformation of the head of the rivet

the robot must perform two tasks:

- Position the end effector (pneumatic hammer) on the head of the rivet perpendicular to the part to be riveted
- Generate a series of shocks on the rivet by the hammer

In the first task, we will check the dynamics of the robot while the robot moves to position the hammer on the rivet head.

In The second task, the robot will deform the head of the rivet, the robot will be exposed to shock vibrations, hence the need to study the vibratory behavior of the robot

To conduct these studies, it is necessary to select the robot suitable for these operations.

II.2 Choice of the robot and its associated models

In robotics, the description of the movement of a manipulator robot in space is carried out by models that allow the passage from the articular space to the operational space and vice versa. Among these models, we distinguish:

- Direct and inverse geometric models that express the situation of the end effector as a function of the configuration of the mechanism and vice versa.
- Direct and inverse kinematic models that express the speed of the end effector as a function of the joint speed and vice versa.
- Dynamic models defining the equations of motion of the robot, which make it possible to establish the relationships between the torques or forces exerted by the actuators and the positions, speeds and accelerations of the joints. [18]

The task will be entrusted to the six-axis robot manipulator Rx90 whose joints 4 and 6 are blocked (Figure II.3).

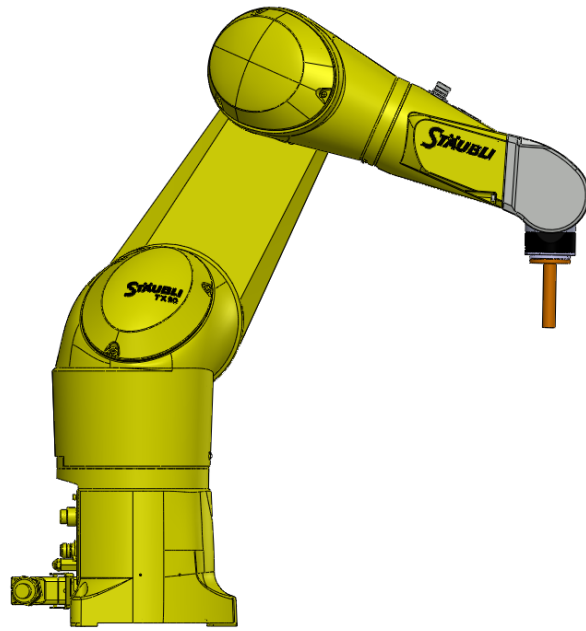


Figure II.3 ROBOT Staubli RX90 six axes

the geometric model thus obtained has the structure of an open articulated chain (Figure 2.4).

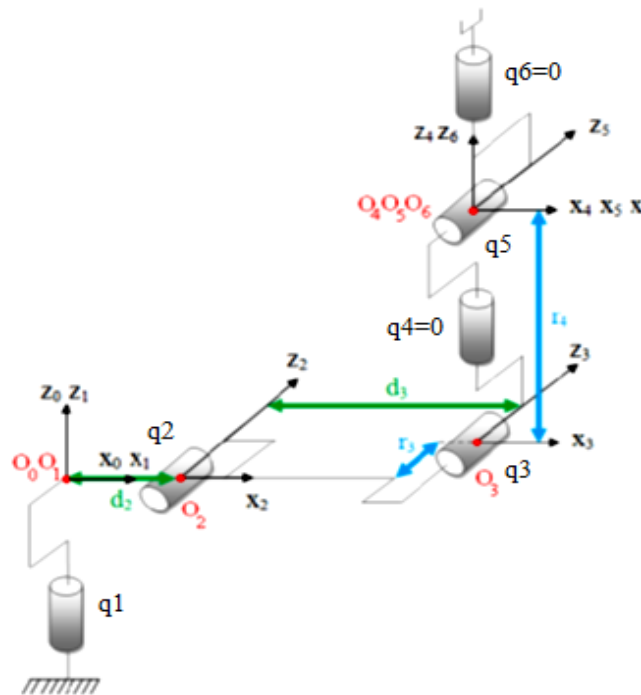


Figure II.4 “Geometric” zero configuration

II.3 Geometric model:

The choice of parameters is an essential step to study the system, the parameterization of Denavit Hartenberg is the most adequate for simple open chain robots

A. Denavit-Hartenberg settings:

The geometry of the robot is described in the position where all the axes are at zero. The method used to describe the robot's morphology is the modified Denavit-Hartenberg method [13]. In figure II.2, we demonstrate the Denavit-Hartenberg parameter.

Reference is made to figure 2.5 we note :

Z_j : Carried by the axis of joint j

X_j : Carried by the common perpendicular to Z_j and Z_{j+1}

R_j : A frame related to the body C_j , at the origin O_j , defined by

$$R_j = \{O_j X_j Y_j Z_j \} \quad (2.1)$$

One defines 4 geometrical parameters which allow the passage of the reference R_{j-1} to the reference R_j :

- α_j : The angle between Z_{j-1} and Z_j corresponding to a rotation around X_{j-1} .
- d_j : The distance between Z_{j-1} and Z_j along X_{j-1} .
- θ_j : The angle between the axes X_{j-1} and X_j corresponding to a rotation around , Z_j

$\text{Rot}(Z, \theta)$

- r_j : The distance between X_{j-1} and X_j along .

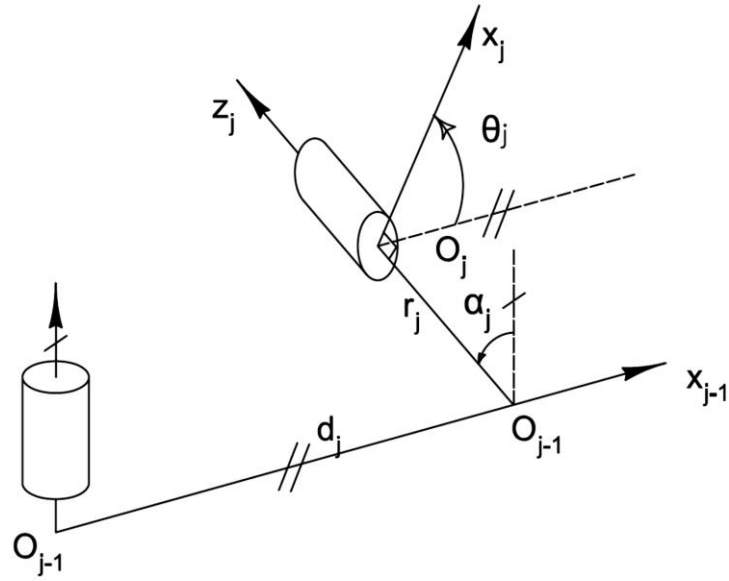


Figure II.5 Geometric parameters in the case of a simple open structure

We associate the joint variable q_j with the j ème joint ($j = 1, \dots, 4$):

$$q_j = \bar{\sigma}_j \cdot \theta_j + \bar{\sigma}_j \cdot r_j \quad (2.2)$$

$\bar{\sigma}_j$: defines the type of joint j :

- $\bar{\sigma}_j = 0$ if joint j is rotoid.
- $\bar{\sigma}_j = 1$ if joint j is prismatic.
- $\bar{\sigma}_j = 2$ if joint j is fixed. [20]

In our case, $q_j = \theta_j$ ($\bar{\sigma}_j = 0$) because the 6 joints are rotoidal and we note :

$$q = [\theta_1 \theta_2 \theta_3 \theta_4 \theta_5 \theta_6]^T \quad (2.3)$$

The geometric dimensions of the Stäubli TX-90 are shown in Figure II.6 and the Denavit-Hartenberg parameters in Table II.1. The distribution of the amplitudes is shown in Table II.2.

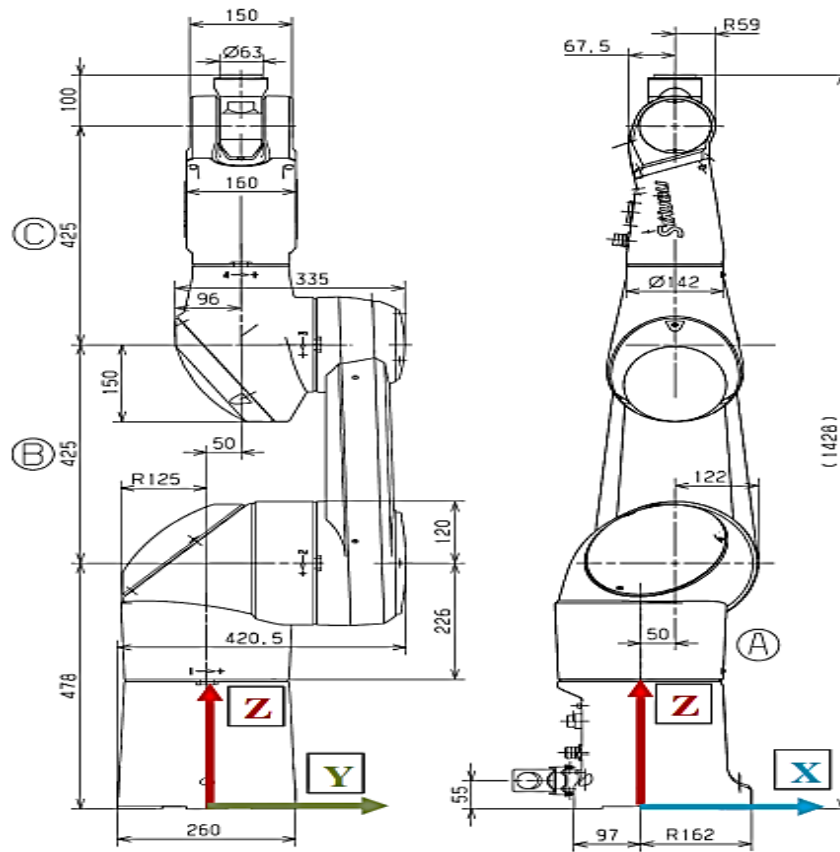


Figure II.6 Geometric dimensions of the StaublitX-90 robot

The Denavit-Hartenberg parameters thus chosen are in Table II.1

j	σ_j	α_j	d_j	θ_j	r_j
1	0	0	0	θ_1	0
2	0	$-\pi/2$	$d_2=50mm$	θ_2	0
3	0	0	$d_3=425mm$	θ_3	$r_3=50mm$
4	0	$\pi/2$	0	0	$r_4=425mm$
5	0	$-\pi/2$	0	θ_5	0
6	0	$\pi/2$	0	0	0

Table II.1 Denavit-Hartenberg (D-H) parameters of the StaublitX-90

The maximum deflections of the StaublitX-90 robot are shown in Table II.2

θ_j	$\theta_j \text{ min } (^\circ)$	$\theta_j \text{ max } (^\circ)$
θ_1	-180	+180
θ_2	-130	+147.5
θ_3	-145	+145
θ_4	0	0
θ_5	-115	+140
θ_6	0	0

Table II.2 TX-90 Rotation deflections

B. Transformation matrix:

The matrix of homogeneous transformation ${}^{j-1}T_j$ which represents the matrix of passage between two consecutive reference marks R_j in R_{j-1} ($j=1, \dots, 6$) is defined by:

$${}^{j-1}T_j = \text{Rot}(x, \alpha_j) \text{Trans}(x, d_j) \text{Rot}(z, \theta_j) \text{Trans}(z, r_j) \quad (2.4)$$

$${}^{j-1}T_j = \begin{bmatrix} C\theta_j & -S\theta_j & 0 & d_j \\ C\alpha_j S\theta_j & C\alpha_j C\theta_j & -S\alpha_j & -r_j S\alpha_j \\ S\alpha_j S\theta_j & S\alpha_j C\theta_j & C\alpha_j & r_j C\alpha_j \\ 0 & 0 & 0 & 1 \end{bmatrix} = \begin{bmatrix} {}^{j-1}A_j & {}^{j-1}P_j \\ 0 & 0 & 0 & 1 \end{bmatrix} \quad (2.5)$$

With :

$$C\theta_j = \cos \theta_j, S\theta_j = \sin \theta_j, C\alpha_j = \cos \alpha_j, S\alpha_j = \sin \alpha_j$$

II.3.1 Direct geometric model (DGM) :

Thus the geometric model that allows the passage from the articular space to the operational space is the DGM which is a generalized function of coordinates.

$$[X] = [T(q)] \quad (2.6)$$

With :

$$q = [\theta_1 \ \theta_2 \ \theta_3 \ \theta_4 \ \theta_5 \ \theta_6]^T \quad (2.7)$$

The matrix $T(q)$ is composed of:

➤ The position is described by the Cartesian coordinates: ${}^0P_6 = [P_x \ P_y \ P_z]^T$ (2.8)

➤ The orientation is described through the following representation: ${}^0R_6 = [{}^0s_6 \ {}^0n_6 \ {}^0a_6]^T$ (2.9)

In the case of a simple open chain, the calculation of the DGM leads to identifying the transformation matrix between ${}^0T_6 R_0$ and R_6 . To do this, the following successive calculations are carried out:

$${}^0T_6 = {}^0T_1 \cdot {}^1T_2 \cdot {}^2T_3 \cdot {}^3T_4 \cdot {}^4T_5 \cdot {}^5T_6 \quad (2.10)$$

The transformation matrices of the TX90 modify for $j = 1, \dots, 6$ which derives from the DGM are as follows:

$$\theta_4 = 0, \theta_6 = 0.$$

$$\begin{aligned} {}^0T_1 &= \begin{bmatrix} C1 & -S1 & 0 & 0 \\ S1 & C1 & 0 & 0 \\ 0 & 0 & 1 & 0 \\ 0 & 0 & 0 & 1 \end{bmatrix} & {}^1T_2 &= \begin{bmatrix} C2 & -S2 & 0 & d2 \\ 0 & 0 & 1 & 0 \\ -S2 & -C2 & 0 & 0 \\ 0 & 0 & 0 & 1 \end{bmatrix} \\ {}^2T_3 &= \begin{bmatrix} C3 & -S3 & 0 & d3 \\ S3 & C3 & 0 & 0 \\ 0 & 0 & 1 & r3 \\ 0 & 0 & 0 & 1 \end{bmatrix} & {}^3T_4 &= \begin{bmatrix} 1 & 0 & 0 & 0 \\ 0 & 0 & -1 & -r4 \\ 0 & 1 & 0 & 0 \\ 0 & 0 & 0 & 1 \end{bmatrix} \\ {}^4T_5 &= \begin{bmatrix} C5 & -S5 & 0 & 0 \\ 0 & 0 & 1 & 0 \\ -S5 & -C5 & 0 & 0 \\ 0 & 0 & 0 & 1 \end{bmatrix} & {}^5T_6 &= \begin{bmatrix} 1 & 0 & 0 & 0 \\ 0 & 0 & -1 & 0 \\ 0 & 1 & 0 & 0 \\ 0 & 0 & 0 & 1 \end{bmatrix} \end{aligned} \quad (2.11)$$

Tool matrix :

$${}^6T_E = \begin{bmatrix} 1 & 0 & 0 & 0 \\ 0 & 1 & 0 & 0 \\ 0 & 0 & 1 & 0.2 \\ 0 & 0 & 0 & 1 \end{bmatrix} \quad (2.12)$$

$$\text{Finally : } {}^0T_6 = \begin{bmatrix} s_x & n_x & a_x & P_x \\ s_y & n_y & a_y & P_y \\ s_z & n_z & a_z & P_x \\ 0 & 0 & 0 & 1 \end{bmatrix} = \begin{bmatrix} & & & \\ & {}^0A_6 & & {}^0P_6 \\ 0 & 0 & 0 & 1 \end{bmatrix} \quad (2.13)$$

With:

$$s_x = C1.(C23.(C5) - S23.S5)$$

$$n_x = -S1$$

$$a_x = C1.(C23.S5 + S23.C5)$$

$$P_x = C1.(S23.r_4 + d_2 + d_3.C2) - S1.r_3$$

$$s_y = S1.(C23.(C5) - S23.S5)$$

$$n_y = C1$$

$$a_y = S1.(C23.S5 + S23.C5)$$

$$P_y = S1.(S23.r_4 + d_2 + d_3 .C2) + C1. r_3$$

$$s_z = -S23.(C5) - C23.S5$$

$$n_z = 0$$

$$a_z = -S23.S5 + C23.C5$$

$$P_z = C23.r_4 - d_3 .S2$$

II.3.2 Inverse Geometric Model (IGM):

The opposite problem consists in calculating the joint coordinates corresponding to a desired situation of the end effector. That is to say, starting from the position of the end effector in the matrix 0T_6 , the values of the articular variables are sought. When they exist, the explicit form that gives all the possible solutions (there is rarely a uniqueness of solution) constitutes what is called the inverse geometric model (IGM).

Note that by calculating the IGM, we can obtain several possible solutions, because there is no single solution (there is not a single joint configuration for each Cartesian position), unlike the direct geometric model (DGM). The number of possible solutions corresponding to the TX-90 is eight [Figure II.7].

$$q = f'(X) ; q = [\theta_1 \theta_2 \theta_3 \theta_4 \theta_5 \theta_6]^T \quad (2.14)$$

Three methods of calculating the MGI can be distinguished [13]:

Paul's method that treats each particular case separately and is suitable for most industrial robots.

This method can also be applied to a robot of the same morphology as the Staubli TX-90 robot of 4 joints, 3 joints for positioning and one joint for orientation.

Before solving an IGM, you must check the following 2 conditions:

- ❖ Check that the desired situation is in the accessible area of the robot, otherwise we will not have a real solution to the IGM.
- ❖ Avoid singular configurations so as not to have an infinite number of solutions to IGM. The singularities of the wearer and of the wrist of the TX-90 will be represented, hereinafter, by the conditions of existence of the various solutions θ_j ($j=1, \dots, 6$) of the IGM.

Application of Paul's method:

Paul's method consists in pre-multiplying, successively, the two members of the equation by ${}^jT_{j-1}$ for j varying from 1 to $n-1$, ($j=1, \dots, n-1$) which makes it possible to calculate, successively, the variables q_j .

We are looking to solve:

$$U_0 = {}^0T_1(q_1). {}^1T_2(q_2). {}^2T_3(q_3). {}^3T_4(q_4). {}^4T_5(q_5). {}^5T_6(q_6) \quad (2.15)$$

The structure of the TX-90 ensures position/orientation decoupling at the point of intersection of the last 3 axes ($O_4=O_5=O_6$). The problem therefore comes down to solving positional equations:

U_0 is the desired situation of the robot, such as :

$$U_0 = {}^0T_6 = \begin{bmatrix} & {}^0A_6 & & {}^0P_6 \\ 0 & 0 & 0 & 1 \end{bmatrix} \quad (2.16)$$

Positional equations:

Since ${}^0P_6 = {}^0P_4$, we can write the fourth column of the product of transformations ${}^0T_1. {}^1T_2. {}^2T_3. {}^3T_4$ is equal to the fourth column of U_0 that is :

$$\Rightarrow \begin{bmatrix} P_x \\ P_y \\ P_z \\ 1 \end{bmatrix} = {}^0T_4 \cdot \begin{bmatrix} 0 \\ 0 \\ 0 \\ 1 \end{bmatrix} = {}^0T_1. {}^1T_2. {}^2T_3. {}^3T_4 \cdot \begin{bmatrix} 0 \\ 0 \\ 0 \\ 1 \end{bmatrix} \quad (2.17)$$

The variables $(\theta_1, \theta_2, \theta_3)$ are solved on the basis of this system of equations by successively pre-multiplying the two limbs by jT_0 ($j=1, 2, \dots$) to isolate and identify the articular variables. The elements of the second member have already been calculated during the establishment of the DGM if the precaution of starting the multiplications has been taken transformation matrices starting from the end of the manipulator [18]

Resolution of θ_1 :

$$\begin{cases} S1 = \frac{-(P_x).r_3 + (P_y).\sqrt{P_x^2 + P_y^2 - r_3^2}}{P_x^2 + P_y^2} \\ C1 = \frac{(P_y).r_3 - (-P_x).\sqrt{P_x^2 + P_y^2 - r_3^2}}{P_x^2 + P_y^2} \end{cases} \quad (2.18)$$

$$\theta_1 = \text{atan2}(S_1, C_1)$$

Résolution of θ_2 :

$$B = C1.P_x + S1.P_y - d_2$$

$$X = -2.P_z.d_3$$

$$Y = 2.B.d_3$$

$$Z = B^2 + P_z^2 + d_3^2 - r_4^2$$

$$\begin{cases} S2 = \frac{X.Z + \varepsilon.Y.\sqrt{X^2 + Y^2 - Z^2}}{X^2 + Y^2} \\ C2 = \frac{Y.Z - \varepsilon.X.\sqrt{X^2 + Y^2 - Z^2}}{X^2 + Y^2} \end{cases} \text{ avec : } \varepsilon \pm 1 \quad (2.19)$$

$$\theta_2 = \text{atan2}(Z, \sqrt{X^2 + Y^2 - Z^2}) - \text{atan2}(Y, X)$$

$$\theta_2 = \text{atan2}(S2, C2)$$

Resolution of θ_3 :

$$\begin{cases} S3 = C2.B - S2.P_z - d_3 \\ C3 = S2.B + C2.P_z \end{cases} \quad (2.20)$$

$$\theta_3 = \text{atan2}(S3, C3)$$

Orientation equation :

The orientation of U_0 is given by :

$${}^0 A_6 = [s \quad n \quad a]$$

$$s = [s_x \quad s_y \quad s_z]^T$$

$$n = [n_x \quad n_y \quad n_z]^T$$

$$a = [a_x \quad a_y \quad a_z]^T$$

We pre-multiply the 2 members by ${}^3 A_0$, we'll get :

$${}^3 A_0(\theta_1, \theta_2, \theta_3).[s \quad n \quad a] = {}^3 A_6(\theta_4, \theta_5, \theta_6)$$

$${}^3 A_0(\theta_1, \theta_2, \theta_3).[s \quad n \quad a] = \begin{bmatrix} F_x & G_x & H_x \\ F_y & G_y & H_y \\ F_z & G_z & H_z \end{bmatrix}$$

Which is equivalent to :

$$[F \quad G \quad H] = {}^3 A_6(\theta_4, \theta_5, \theta_6) \quad (2.21)$$

$$F = [F_x, F_y, F_z]^T$$

$$F = [C23. (C1. s_x + S1. s_y) - S23. s_z, -S23. (C1. s_x + S1. s_y) - C23. s_z, -S1. s_x + C1. s_y]^T$$

$$G = [G_x, G_y, G_z]^T$$

$$G = [C23. (C1. n_x + S1. n_y) - S23. n_z, -S23. (C1. n_x + S1. n_y) - C23. n_z, -S1. n_x + C1. n_y]^T$$

$$H = [H_x, H_y, H_z]^T$$

$$H = [C23. (C1. a_x + S1. a_y) - S23. a_z, -S23. (C1. a_x + S1. a_y) - C23. a_z, -S1. a_x + C1. a_y]^T$$

Since the variables ($\theta_1, \theta_2, \theta_3$) are known, it is sufficient to pre-multiply the two 2 members of the equation by 4A_3 . We identify, term by term, the two members. We will have 3 systems of equations that will allow us to have successively θ_4, θ_5 and θ_6 such that:

Resolution of θ_4 :

$$\theta_4 = 0$$

Resolution of θ_5 :

$$H_y = -S23. (C1. a_x + S1. a_y) - C23. a_z$$

$$\begin{cases} S5 = C4. H_x + S4. H_z \\ C5 = -H_y \end{cases} \quad \text{avec } C4 = 1 \text{ et } S4 = 0$$

$$\begin{cases} S5 = H_x \\ C5 = -H_y \end{cases} \quad (2.22)$$

$$\theta_5 = \text{atan2}(S5, C5)$$

Resolution of θ_6 :

$$\theta_6 = 0$$

The exploitation of the IGM silutions can be represented by figure II.7

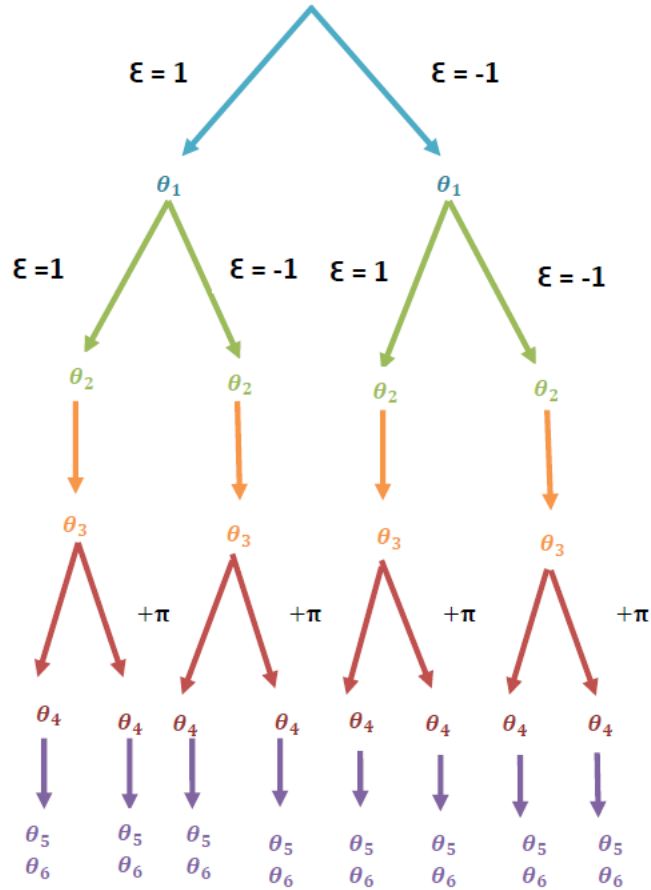


Figure II.7 8 solutions possibles for IGM of TX 90

With : $\theta_4=0$ et $\theta_6=0$

II.4 kinematic model :

The Direct Kinematic Model (DKM) of a manipulator robot describes the velocities of operational coordinates according to joint velocities.

$$\dot{X}=J(q). \dot{q}=\begin{bmatrix} V^n \\ \omega^n \end{bmatrix} \quad (2.23)$$

$J(q)$: denotes the Jacobian matrix of the mechanism of dimension $(m \times n)$, equal to $\partial X/\partial q$.

v_n : denotes the speed of translation of the body n in the frame R_0 , equal to the derivative with respect to time of the vector 0P_n ;

ω_n : denotes the rotational speed of the body n in the frame R_0 , but is not equal to the derivative of the orientation settings.[13]

II.4.1 Methods for calculating the Jacobian matrix:

1/We can calculate the Jacobian matrix by deriving the MGD .

$$J_{ij} = \frac{\partial f_i(q)}{\partial q_j} \quad i=1, \dots, m ; j=1, \dots, n \quad (2.24)$$

where J_{ij} : is the element (i, j) of the Jacobian matrix J

This method is avoided because its calculation is long and difficult to implement for the TX-90 which has 6 d.d.d.l. It also assumes that the relationship between the angular velocity and the derivative of the parameters representing the angular configuration is introduced.

2/ The second method consists in calculating the basic Jacobian matrix which is more practical in the case of the TX-90. this direct calculation method based on the relationship between the translation and rotation speed vectors V_n and ω_n of the coordinate system R_n , representing the reduction elements of the kinematic torsor of the coordinate system R_n , and the speeds articular \dot{q} [13]

$$\dot{X} = \begin{bmatrix} V_n \\ \omega_n \end{bmatrix} = J_n \cdot \dot{q} = J_n \cdot \dot{\theta} \quad (2.25)$$

Basic jacobienne calculation :

$$\begin{cases} V_{k,n} = (\sigma_k a_k + \bar{\sigma}_k (a_k \wedge L_{k,n})) \dot{q}_k \\ \omega_{k,n} = \bar{\sigma}_k a_k \dot{q}_k \end{cases} \quad (2.26)$$

$$\begin{cases} V_n = \sum_{k=1}^n V_{k,n} = \sum_{k=1}^n [\sigma_k a_k + \bar{\sigma}_k (a_k \wedge L_{k,n})] \dot{q}_k \\ \omega_n = \sum_{k=1}^n \omega_{k,n} = \sum_{k=1}^n \bar{\sigma}_k a_k \dot{q}_k \end{cases} \quad (2.27)$$

Be :

- k : the index of the $k^{ième}$ joint of the robot
- $V_{k,n}$ et $\omega_{k,n}$ the translation and rotation speeds induced by the speed \dot{q}_k on the terminal coordinate system R_n .
- $L_{k,n}$ designates the origin vector O_k and the end vector O_n .
- a_k is the unit vector carried by the axis Z_k of the joint k.
- $\sigma_k = 0$ because the joint is rotoid , $\bar{\sigma}_k = 1$

Calculation of matrix ${}^i J_n$:

The vector product $a_k \times L_{k,n}$ can turn into $a_k \wedge L_{k,n}$ la $k^{i\grave{e}me}$ column of ${}^i J_n$ noted ${}^i J_{n,k}$ become :

$${}^i J_{n,k} = \begin{bmatrix} \sigma_k {}^i a_k + \bar{\sigma}_k {}^i A_k \wedge {}^k a_k \wedge {}^k L_{k,n} \\ \bar{\sigma}_k {}^i a_k \end{bmatrix}$$

Expanding on , and noting that :

- ${}^k a_k = [0 \ 0 \ 1]^T$
- ${}^k L_{k,n} = {}^k P_n$

We obtain :

$${}^i J_{n,k} = \begin{bmatrix} \sigma_k {}^i a_k + \bar{\sigma}_k (-{}^k P_{ny} {}^i s_k + {}^k P_{nx} {}^i n_k) \\ \bar{\sigma}_k {}^i a_k \end{bmatrix} \quad (2.28)$$

Where ${}^k P_{nx}$ and ${}^k P_{ny}$ are respectively the x and y components of the vector ${}^k P_n$

${}^0 J_n = {}^0 J_6$. Each column of the matrix ${}^i J_6$ is written (at point O_6 and in the coordinate system R_0) in the following form:

$$J_{6,k} = \begin{bmatrix} -{}^k P_{6y} {}^0 s_k + {}^k P_{6x} {}^0 n_k \\ {}^0 a_k \end{bmatrix} \quad (2.29)$$

We also present the columns of the Jacobian matrix ${}^0 J_6$ of the TX-90 robot:

$$\theta_4=0, \theta_6=0$$

$${}^0 J_{6,1} = \begin{bmatrix} -r_3 \cdot C1 - (S23 \cdot r_4 + d_2 + d_3 \cdot C2) \cdot S1 \\ -r_3 \cdot S1 - (S23 \cdot r_4 + d_2 + d_3 \cdot C2) \cdot C1 \\ 0 \\ 0 \\ 0 \\ 1 \end{bmatrix}$$

$${}^0 J_{6,2} = \begin{bmatrix} C3 \cdot r_4 (C1 \cdot C2) - (S3 \cdot r_4 + d_3) (C1 \cdot S2) \\ C3 \cdot r_4 (S1 \cdot C2) - (S3 \cdot r_4 + d_3) (S1 \cdot S2) \\ -C3 \cdot r_4 \cdot S2 - (S3 \cdot r_4 + d_3) \cdot C2 \\ -S1 \\ C1 \\ 0 \end{bmatrix} \quad (2.30)$$

$${}^0J_{6,3} = \begin{bmatrix} r_4(C1.C2.C3 - C1.S2.S3) \\ r_4(S1.C2.C3 - S1.S2.S3) \\ r_4(-S2.C3 - C2.S3) \\ -S1 \\ C1 \\ 0 \end{bmatrix} \quad {}^0J_{6,4} = \begin{bmatrix} 0 \\ 0 \\ 0 \\ C1.C2.S3 + C1.S2.C3 \\ S1.C2.S3 + S1.S2.C3 \\ -S2.S3 + C2.C3 \end{bmatrix}$$

$${}^0J_{6,5} = \begin{bmatrix} 0 \\ 0 \\ 0 \\ -S1 \\ -C1 \\ 0 \end{bmatrix} \quad {}^0J_{6,6} = \begin{bmatrix} 0 \\ 0 \\ 0 \\ C1(C23.S5 + S23.C5) \\ S1(C23.S5 + S23.C5) \\ -S23.S5 + C23.C5 \end{bmatrix}$$

II.4.2 First Order Inverse Kinematic Model:

The inverse kinematic model of the first order makes it possible to determine the speed of the articular variables \dot{q} as a function of the speed of the operational variables \dot{X}

$$\dot{X} = J(q)\dot{q} \quad (2.31)$$

$$\dot{q} = J^{-1}(q)\dot{X} \quad (2.32)$$

II.4.3 Second Order Inverse Kinematic Model:

Thus, by derivation, of the 2 relations above are deduced in order to obtain the inverse kinematic model of the second order which link the articular and Cartesian accelerations

$$\ddot{X} = J(q)\ddot{q} + j(q, \dot{q})\dot{q} \quad (2.33)$$

$$\ddot{q} = J^{-1}(q)[\ddot{X} - j(q, \dot{q})\dot{q}] \quad (2.34)$$

II.5 The dynamic model :

torques (and/or forces) applied to the actuators and the joint positions, velocities and accelerations. The dynamic model is represented by a relation of the form:

$$\Gamma = f(q, \dot{q}, \ddot{q}, fe) \quad (2.35)$$

With :

Γ : vector of torque/forces of the actuators

q : vector of joint positions

\dot{q} : vector of joint velocities

\ddot{q} : vector of joint accelerations

f_e : vector representing the external force that the robot exerts on the environment ,in our case the external force is zero ($f_e = 0$) .[13]

II.5.1 Inverse dynamic model (IDM):

Both the Lagrange formulation and the Newton–Euler formulation allow the relationship between joint torques and, end-effector forces and motion of the structure to be calculated. A comparison between the two approaches reveals the following. The Lagrange formulation has the following advantages [19] :

- It is systematic and immediately understandable.
- It provides the equations of motion in a compact analytical form containing the matrix of inertia, the matrix of centrifugal and Coriolis forces, and the vector of gravitational forces. Such a shape is advantageous for control design.
- It is effective if you want to include more complex mechanical effects such as the deformation of a flexible link.

The Newton–Euler formulation has the following fundamental advantage:

- It is an inherently recursive method that is computationally efficient.

Newton-Euler offers the possibility of obtaining the dynamic model by means of symbolic calculation and without going through numerical derivation.

In the study of dynamics, it is relevant to find a solution to two types of problems concerning the calculation of forward dynamics and inverse dynamics. The direct dynamics problem consists in determining, for $t > t_0$, the joint accelerations $\ddot{q}(t)$ (and therefore $\dot{q}(t)$, $q(t)$) resulting from the given joint torques $\tau(t)$ and the forces applied on the terminal device once the initial positions $q(t_0)$ and the velocities $\dot{q}(t_0)$ are known (initial state of the system).

The inverse dynamics problem consists in determining the joint torques $\tau(t)$ necessary to generate the movement specified by the joint accelerations $\ddot{q}(t)$, the velocities $\dot{q}(t)$ and the positions $q(t)$ once the forces are applied are known. [19]

The Newton Euler's formalism :

In this section, we develop the Newton-Euler algorithm based on the double recursive computations of Luh *and al.*

Newtonian-Euler mechanics is based on the following principles:

Every action has an equal and opposite reaction. Thus, if a body 1 applies a force \vec{f} and a torque $\vec{\tau}$ on body 2, then, body 2 applies a force $-\vec{f}$ and a torque $-\vec{\tau}$ on body 1.

The change in momentum is equal to the sum of the total forces applied to the body.

The variation of the kinetic torque is equal to all the torques applied to the body.

Newton Euler double recursive algorithm based on Luh's method and other. This algorithm For our Application, we used Newton Euler's double recursive algorithm based on Luh's method. This algorithm expresses the dynamic torsor of the external forces applied to the center of gravity of the body i . Using the inertial parameters m_i , S_i and I_i it is possible to write the algorithm:

forward recurrence for $i=1, \dots, n$ (Fig III.8) expresses the dynamic torsor of the external forces applied to the center of the reference frame of the body i . Using the inertial parameters m_i , S_i and I_i it is possible to write the algorithm:

forward recursive for $i=1, \dots, n$ (Fig III.8).

The speeds and accelerations are calculated starting from the base towards the terminal organ that allows to find the vector τ of couples to the actuators necessary to respond to a trajectory of which q , \dot{q} and \ddot{q} are given.

This model is the most used in the world of robotics because the robot is controlled by its joint variables q , \dot{q} and \ddot{q} and we seek to find the torques Γ at the level of the joints. The formalisms used to calculate this model are numerous [Gautier 1990] (Lagrange formalism, Newton-Euler formalism, etc.). [13]

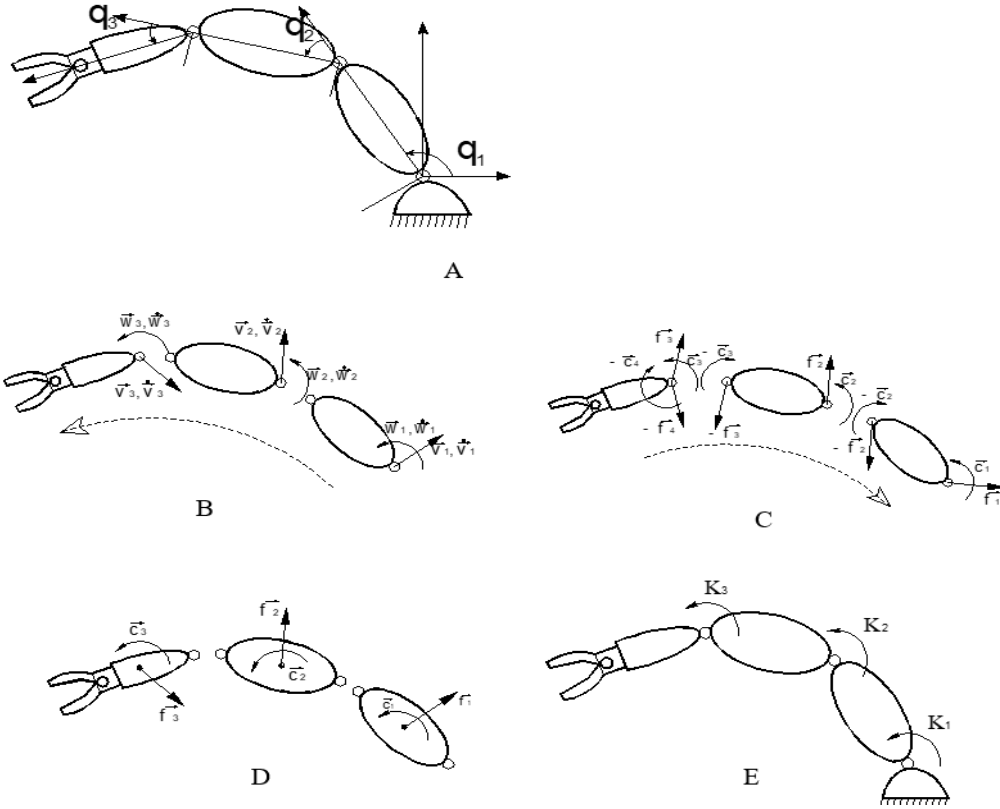


Figure II.8 Assessment of forces, speeds and accelerations

In the context of this thesis, we have chosen to use the formalism which is based on the **Newton-Euler** equations.

The Eulerian formalism describes the motion of a solid as a function of its kinematic velocity torsor $[V^T \ \omega^T]^T$. The Newton-Euler equations of a body C_j express the equality between the dynamic torsor and the torsor of the external forces on a body j at its center of gravity G_j , including the effect of gravity. However, expressing the dynamic torsor at the origin O_j of the reference body j rather than at the point G_j , makes it possible to have a linear dynamic model with respect to the inertial parameters. [20] , [13] The equations are then the following:

$$F_j = M_j \dot{V}_j + \dot{\omega}_j \times M S_j + \omega_j \times (\omega_j \times M S_j) \quad (2.36)$$

$$M_j = J_j \dot{\omega}_j + \omega_j \times (J_j \omega_j) + M S_j \times \dot{V}_j \quad (2.37)$$

With :

M_j is the moment of the external forces applied to the body C_j at its origin O_j ;

F_j is the resultant of the external forces applied to the body j ;

ω_j is the rotational acceleration vector of body j ;

It is noted that the model in Lagrangian variables can be obtained from the Newton–Euler equations by expressing the velocity and acceleration torsors as a function of the joint variables and its derivatives without explicitly calculating the matrices A , C and G .

The method of Luh, Walker and Paul makes it possible to calculate the dynamic model of a robot by a double recurrence:

- i) A forward recurrence, from the base of the robot to the effector, which successively calculates the velocities and accelerations of the bodies, then their dynamic torsors.
- ii) A backward recurrence, from the end-effector towards the base, which calculates the articular forces by considering the external forces applied to the robot and the articular forces in the equilibrium equation of each body.

Recurrence before It is used to calculate the dynamic torque from the following equations:

For $j=1 \dots n$

For a fixed base robot, the initialization of this recurrence is:

starting from the base to the end effector :

$${}^0\omega_0 = [0 \ 0 \ 0]^T, {}^0\dot{\omega}_0 = [0 \ 0 \ 0]^T, {}^0\dot{V}_0 = [0 \ 0 \ 0]^T$$

$${}^j\omega_{j-1} = {}^jA_{j-1} {}^{j-1}\omega_{j-1} \quad (2.38)$$

$${}^j\omega_j = {}^j\omega_{j-1} + \bar{\sigma}_j \dot{q}_j {}^j a_j \quad (2.39)$$

$${}^j\dot{\omega}_j = {}^jA_{j-1} {}^{j-1}\dot{\omega}_{j-1} + \bar{\sigma}_j [\ddot{q}_j {}^j a_j + {}^j\omega_{j-1} \times \dot{q}_j {}^j a_j] \quad (2.40)$$

$${}^j\dot{V}_j = {}^jA_{j-1} ({}^{j-1}\dot{V}_{j-1} + {}^{j-1}U_{j-1} {}^{j-1}P_j) + \sigma_j (\ddot{q}_j {}^j a_j + 2 {}^j\omega_{j-1} \times \dot{q}_j {}^j a_j) \quad (2.41)$$

$${}^jF_j = M_j {}^j\dot{V}_j + {}^jU_j {}^jMS_j \quad (2.42)$$

$${}^jM_j = {}^jJ_j {}^j\dot{\omega}_j + {}^i\omega_j \times ({}^jJ_j {}^j\omega_j) + {}^jMS_j \times {}^j\dot{V}_j \quad (2.43)$$

With :

Sj the coordinates of the point Gj in Rj such that $S_j = O_j G_j = [x_G \ y_G \ z_G]^T$

$${}^j U_j = {}^j \hat{\omega}_j + {}^j \hat{\omega}_j \cdot {}^j \hat{\omega}_j \quad (2.44)$$

With:

$\hat{\omega}$: la matrice pré-produit vectorielle

$$\hat{\omega} = \begin{bmatrix} 0 & -\omega_z & \omega_y \\ \omega_z & 0 & -\omega_x \\ -\omega_y & \omega_x & 0 \end{bmatrix} \quad (2.45)$$

The 2nd path, starting from the end effector to the base by calculating the forces and torsors applied to each body.

$${}^j f_j = {}^j F_j + {}^j f_{j+1} + {}^j f_{ej} \quad (2.46)$$

$${}^{j-1} f_j = {}^{j-1} A_j {}^j f_j \quad (2.47)$$

$${}^j m_j = {}^j M_j + {}^j A_{j+1} {}^{j+1} m_{j+1} + {}^j P_{j+1} \times {}^j f_{j+1} + {}^j m_{ej} \quad (2.48)$$

The forces of gravity are calculated by including the acceleration of gravity in the acceleration of each body, which amounts to taking:

$${}^0 \dot{V}_0 = -g \quad (2.49)$$

With:

g is the acceleration vector due to gravity expressed in the reference R0 The joint torques Γ_j are calculated by projecting, depending on the nature of the joint j, the vectors f_j or m_j on the axis of movement.

$$\Gamma_j = (\sigma_j {}^j f_j + \bar{\sigma}_j {}^j m_j)^T {}^j a_j \quad (2.50)$$

With:

${}^j f_j$: the resultant of the forces applied by the antecedent body of index a(j) on the body j

${}^j m_j$: the resultant of the torques applied by the antecedent body with index a(j) on body j

The equation of the actuation chain which considers the effect of friction, of the inertias of the actuators brought back to the load side, is written:

$$\Gamma_j = (\sigma_j f_j + \bar{\sigma}_j m_j)^T {}^j a_j + F_{S_j} \text{Sign}(\dot{q}_j) + F_{V_j} \dot{q}_j + I a_j \ddot{q}_j \quad (2.51)$$

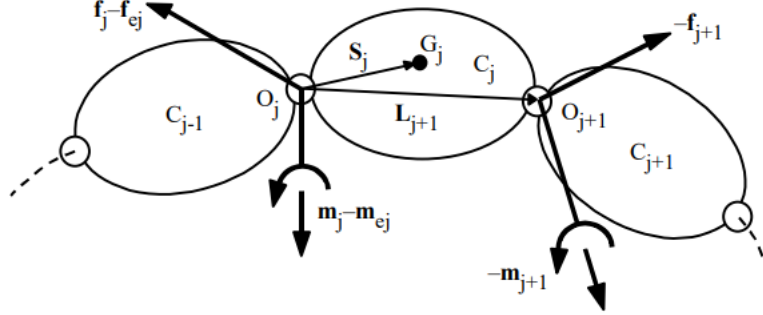


Figure II.9 Forces and moments on link

Algorithme for calculating actuator forces (NE) :

Read the settings

$$m_i, S_i, I_i, I a_i g = [0,0,9.85]$$

$$R_{i+1}^i, P_{i+1}^i, \vec{q}, \dot{\vec{q}}, \ddot{\vec{q}}$$

Initialization

$$\vec{\omega}_0^0 = [0,0,0]^T, \dot{\vec{\omega}}_0^0 = [0,0,0]^T \text{ et } \vec{V}_0^0 = [0,0,0]^T$$

Calculate velocities and accelerations of each body

For $j=1$ to n : dimension of the time vector

For $i=1$ to m : number of bodies

$$\vec{\omega}_{i-1}^i = R_{i-1}^i \vec{\omega}_{i-1}^{i-1}$$

$$\vec{\omega}_i^i = \vec{\omega}_{i-1}^i + \bar{\sigma}_i \dot{q}_i \vec{a}_i^i$$

$$\dot{\vec{\omega}}_i^i = R_{i-1}^i \dot{\vec{\omega}}_{i-1}^{i-1} + \bar{\sigma}_i (\ddot{q}_i \vec{a}_i^i + \vec{\omega}_{i-1}^i \times \dot{q}_i \vec{a}_i^i)$$

$$\dot{\vec{V}}_i^i = R_{i-1}^i \left(\dot{\vec{V}}_{i-1}^{i-1} + \dot{\vec{\omega}}_{i-1}^{i-1} \times \vec{P}_i^{i-1} + \vec{\omega}_{i-1}^{i-1} \times (\vec{\omega}_{i-1}^{i-1} \times \vec{P}_i^{i-1}) \right) + \sigma_i (\ddot{q}_i \vec{a}_i^i + 2\vec{\omega}_{i-1}^i \times \dot{q}_i \vec{a}_i^i)$$

$$F_i^i = m_i \dot{\vec{V}}_i^i + m_i \vec{\omega}_i^i \times \vec{S}_i + \vec{\omega}_i^i \times (\vec{\omega}_i^i \times \vec{S}_i)$$

$$C_i^i = I_i^i \dot{\vec{\omega}}_i^i + \vec{\omega}_i^i \times (I_i^i \vec{\omega}_i^i)$$

End

For $i=m$ to 1 : number of bodies

$$\vec{f}_i^i = \vec{F}_i^i + R_{i+1}^i \vec{f}_{i+1}^{i+1} + R_0^i \vec{g}$$

$$\vec{f}_i^{i-1} = R_i^{i-1} \vec{f}_i^i$$

$$\vec{c}_i^i = \vec{C}_i^i + R_{i+1}^i \vec{c}_{i+1}^{i+1} + \vec{S}_i \wedge \vec{f}_i^i + (\vec{P}_{i+1}^i - \vec{S}_i) \wedge (\vec{f}_{i+1}^{i+1}) + \vec{c}_{ei}^i$$

$$K_i = \left(\sigma_i \vec{f}_i + \bar{\sigma}_i \vec{c}_i \right)^T \vec{a}_i + \vec{F}_{si} \text{Sign}(\dot{q}_i) + \vec{F}_{vi} \dot{q}_i + I_{ai} \ddot{q}_i$$

End

End

Conclusion :

The purpose of this chapter was to introduce the models necessary to carry out this study.

The geometric models express the situation of end effector as a function of the configuration of the mechanism.

Kinematic models make it possible to control the speed of movement of the robot in order to know the duration of execution of the task.

Dynamic models consist in expressing joint accelerations according to the positions, velocities and torques of the joints. It allows to find the vector of couples.

Chapitre III.Natural frequencies ,eignmodes

III.1 Introduction :

An ideal structure is stripped of any damping so that it can vibrate without the need to supply it with energy. This behavior is purely theoretical because of the presence of friction in the material of the structure which dampens the movement of the latter. For most materials, these structural damping are very low, so that the free vibrations persist for quite a long time.

When adequate initial conditions are imposed on the structure, it is possible to cause the structure to vibrate according to any one of these natural modes. The latter are part of the characteristics of the structure. In each natural vibration mode, each point of the structure executes a harmonic movement around its equilibrium position; all the points pass simultaneously through their equilibrium position and through their maximum amplitude. In such a situation, the vibration frequency is the same for all points of the structure and is called the natural frequency relating to the mode of the deformed configuration of the structure. The lowest frequency is said to be: fundamental frequency.

III.2 Resonance :

Resonance is a phenomenon where certain physical systems (electrical, mechanical...) are sensitive to certain frequencies. A resonant system can accumulate energy, if the latter is applied in periodic form, and close to a frequency called resonance frequency, the system will be the seat of increasingly important oscillations, until reaching an equilibrium regime that depends on the dissipative elements of the system, or until a component of the system breaks. or the deterioration of the system.

The critical resonant frequency is the fundamental frequency because the natural mode associated with this frequency does not have any compensation part, hence the excitation of the structure by a force of frequency close to the fundamental frequency of the structure can quickly lead to the destruction of the system or of a part of the system. An elastic structure theoretically has an infinity of eigenmodes of vibration but if it is discretized, the number of eigenmodes is reduced to the number of degrees of freedom.

III.3 Method for calculating frequencies and eigenmodes:

The dynamic model of a non-damped free vibration system is given by :

$$[M]\{\ddot{q}\} + [K]\{q\} = 0 \quad (3.1)$$

Where:

$[M]$ is the inertia matrix and $[K]$ is the stiffness matrix.

It is assumed that the motion of the system is oscillatory, harmonic, the particular solutions can be written in the form :

$$q_i(t) = A_i \sin(\omega t + \varphi) \quad (3.2)$$

$$\text{Et } i = 1, \dots, n$$

Where A_i represents the amplitude , ω is the vibration frequency and φ : the phase

We replace $q_i(t)$ in the motion expression we get:

$$\begin{cases} (K_{11} - M_1\omega^2)A_1 + K_{12}A_2 + \dots + K_{1n}A_n = 0 \\ K_{21}A_1 + (K_{22} - M_2\omega^2)A_2 + \dots + K_{2n}A_n = 0 \\ \dots \\ K_{n1}A_1 + K_{n2}A_2 + \dots + (K_{nn} - M_n\omega^2)A_n = 0 \end{cases} \quad (3.3)$$

The preceding expression can be written in matrix form

$$([K] - \omega^2[M])\{A_i\} \quad (3.4)$$

since :

$\{A\} \neq \{0\}$,in general, the solution of the previous equation:

$$D(\omega) = |[K] - \omega^2[M]| = 0 \quad (3.5)$$

The previous expression represents the characteristic equation of the system, the solution of this equation makes it possible to calculate the eigenvalues of the system , $\lambda = \omega^2$, the system admits an eigenangular frequency ω so $\omega_1 < \omega_2 < \dots \dots \omega_k < \omega_n$.

The smallest value of ω is ω_1 , which is the fundamental pulse.

A pulse of order $i > 1$ is called pulse of order i .

Each eigenvalue corresponds to a form of oscillation. The set of eigenvalues and eigenforms is called (Eigenor or normal mode of vibration).

By replacing the natural frequency ω_i in the previous equation, we get :

$$\begin{aligned}
 (K_{11} - m_1\omega_i^2)A_1 + K_{12}A_2 \cdots \cdots K_{1n}A_n &= 0 \\
 K_{21}A_1 + (K_{22} - m_2\omega_i^2)A_2 \cdots \cdots K_{2n}A_n &= 0 \\
 \cdots \cdots \cdots \cdots \cdots \cdots \cdots \cdots \cdots & \\
 K_{n1}A_1 + K_{n2}A_2 \cdots \cdots \cdots (K_{nn} - m_n\omega_i^2)A_n &= 0
 \end{aligned}
 \tag{3.6}$$

The above system makes it possible to calculate the eigenmodes $\{A_j\}^{(i)}$ which can only be determined in the form of nodal displacement ratio.[21]

The matrices [M] and [K] are very difficult to calculate for a complex system, on the other hand the finite element method is a powerful tool that allows to calculate these matrices for complex structures, in our case, we used the Solidworks software that allows to automatically generate the matrix [M] and [K] and solve the system:

$$[M]\{\ddot{q}\} + [K]\{q\} = 0
 \tag{3.7}$$

To obtain the eigenmodes and eigenfrequencies of the system

II.4 Modeling the force generated by the pneumatic hammer :

Task description: [22]

Applying the pneumatic hammer to the rivet makes it possible to deform the latter plastically (Fig III.1).

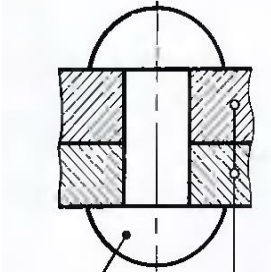


Figure III.1 Parts assembled by the cold-deformed rivet

The phenomenon is very complex, there are several models approached to model the force generated by the pneumatic hammer:

A) Half sinusoid model : [24]

$$x_s(t) = \begin{cases} A \sin\left(\frac{t\pi}{\tau}\right), & 0 \leq t \leq \tau \\ 0, & t > \tau \end{cases} \quad (3.8)$$

where A and τ are amplitude and duration of the shock, respectively .

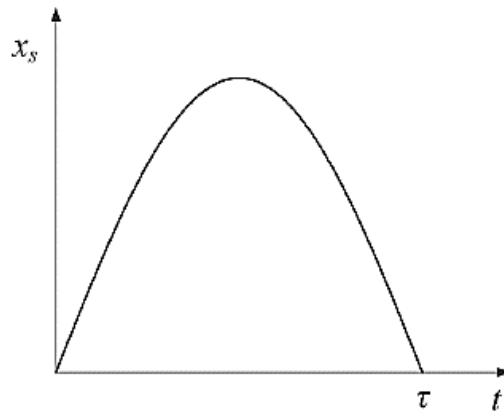


Figure III.2 A choc modeled by a half sinusoid

B) A series of Dirac impulses:

The DIRAC pulse $\delta(t)$ is defined by

$$\int_0^{+\infty} \delta(t) dt = 1 \quad (3.9)$$

A DIRAC pulse is zero everywhere except at $t = t_0$ at a very high value .

C) The unbalance :

The force is modeled by an unbalance defined by the following relation:

$$F = m\omega^2 \sin \omega t \quad (3.10)$$

ω is the frequency of the hammer

M is the mobile mass of the hammer

By consulting the ATLAS COPCO company website, the recommended frequency for a pneumatic riveting tool is:

$$\omega = 3600 \frac{\text{coup}}{\text{min}} = 60 \text{coup/s}$$

The moving mass in the hammer is 1.82 KG

The unbalance force is:

$$F = 6552 \sin 60t \quad (3.11)$$



Figure III.3 Making a joint by rivet manually

The force generated by the hammer can be measured experimentally and in this case, the acceleration of the force is measured as in the case of Figure III.4.

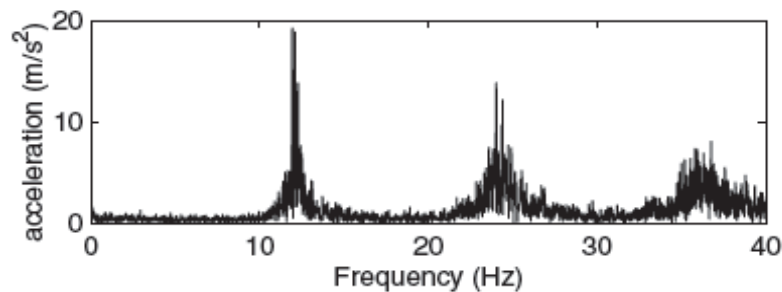


Figure III.4 Acceleration measurement of a pneumatic hammer during the installation of a rivet [23]

Generally speaking, the pneumatic hammer can generate a force with different frequencies going from 10 Hz up to 100 Hz, it remains to define the correct frequency that optimizes the execution time of the riveting operation and the good appearance of the rivet shape.

In our work, we limit ourselves to checking the presence of a resonance during the application of the riveting spot in a frequency range of 10Hz to 100Hz.

Chapter IV : Riveting application

IV.1 Introduction :

Riveting represents a primary joining method for assembling structural components that require high joint strength. Compared to welding which is a method that requires the melting of metals to be assembled, riveting is a mechanical method that generates no thermal deformation, therefore widely used to join materials with high thermal conductivity such as aluminum sheets used in aircraft assembly.

To automate the assembly operation by riveting, we need:

- A robot manipulator robot StäubliX-90 chapter 2
- The rivet chapter 3
- Tool for riveting
- Work environment

IV.2 The rivet :

The rivets that will be used in this study have domed heads of aluminum material that can be deformed by strikes (Fig IV.1). The use of this type of rivets requires a tool similar to the one used manually for the deformation of the second head.

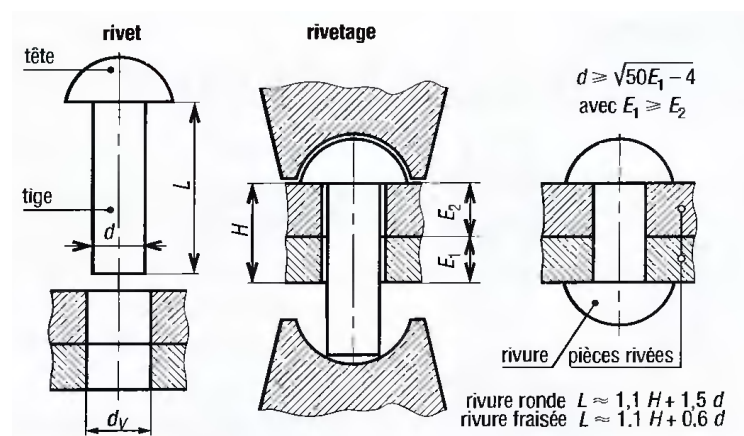


Figure IV.1 Deformable toe rivet

IV.3 Riveting tool :

The tool is a system composed of 3 parts (FigIV.2 ,Fig IV.3, Fig IV.4)

The first part is a cylinder composed of a fixing device on the end effector , we can find two holes that allow the entry and the escape of air.

The second part is a piston that can slide inside the cylinder, the executive end is composed of a recess that makes it possible to give the curved shape of the rivet.

The third part is a spring that ensures the return of the piston after the air has escaped.

The system is made of hard steel.

The cylinder and the piston are made of : Z 200

The spring is made of : Spring steel .

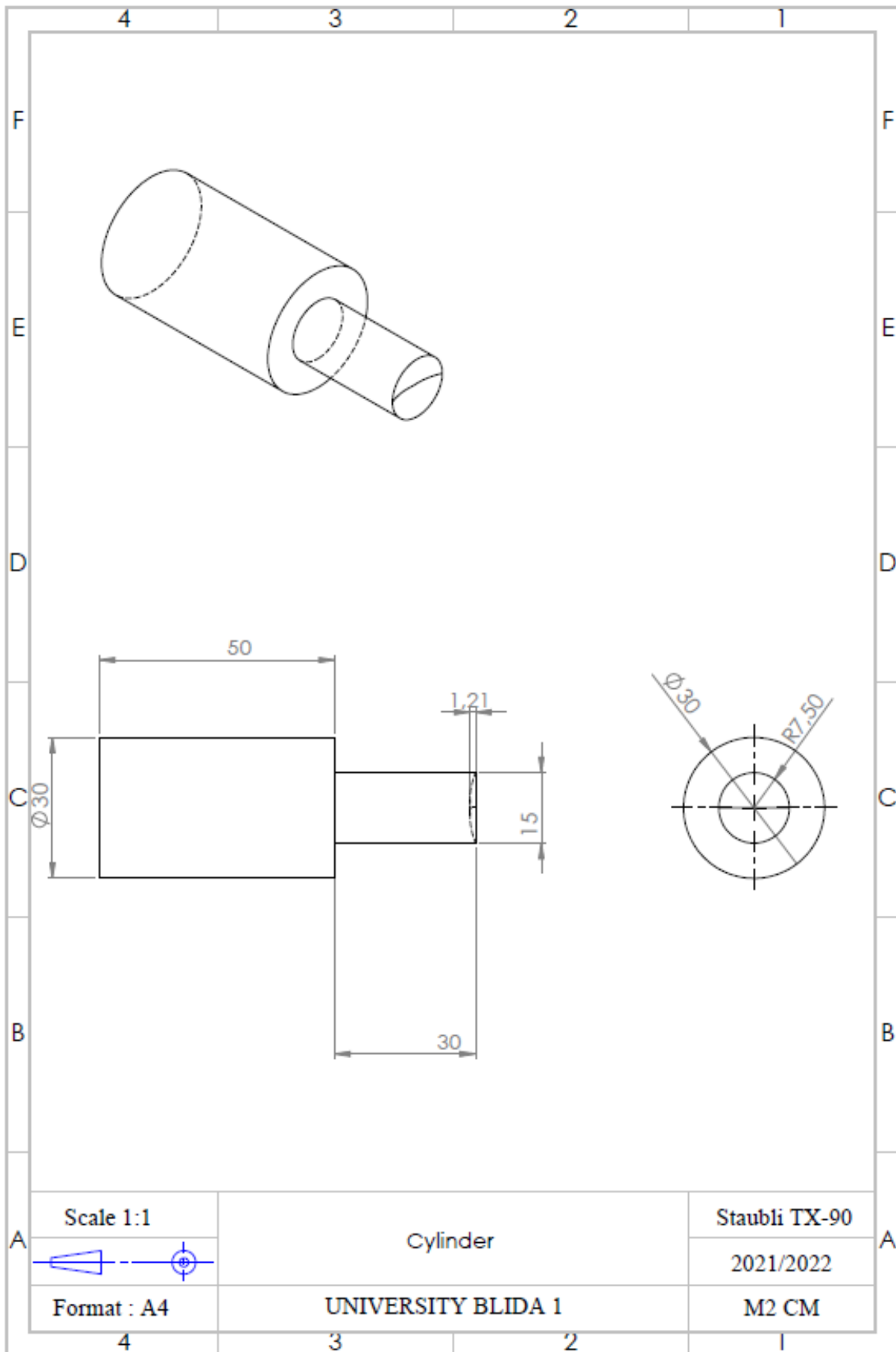


Figure IV.2 The cylinder

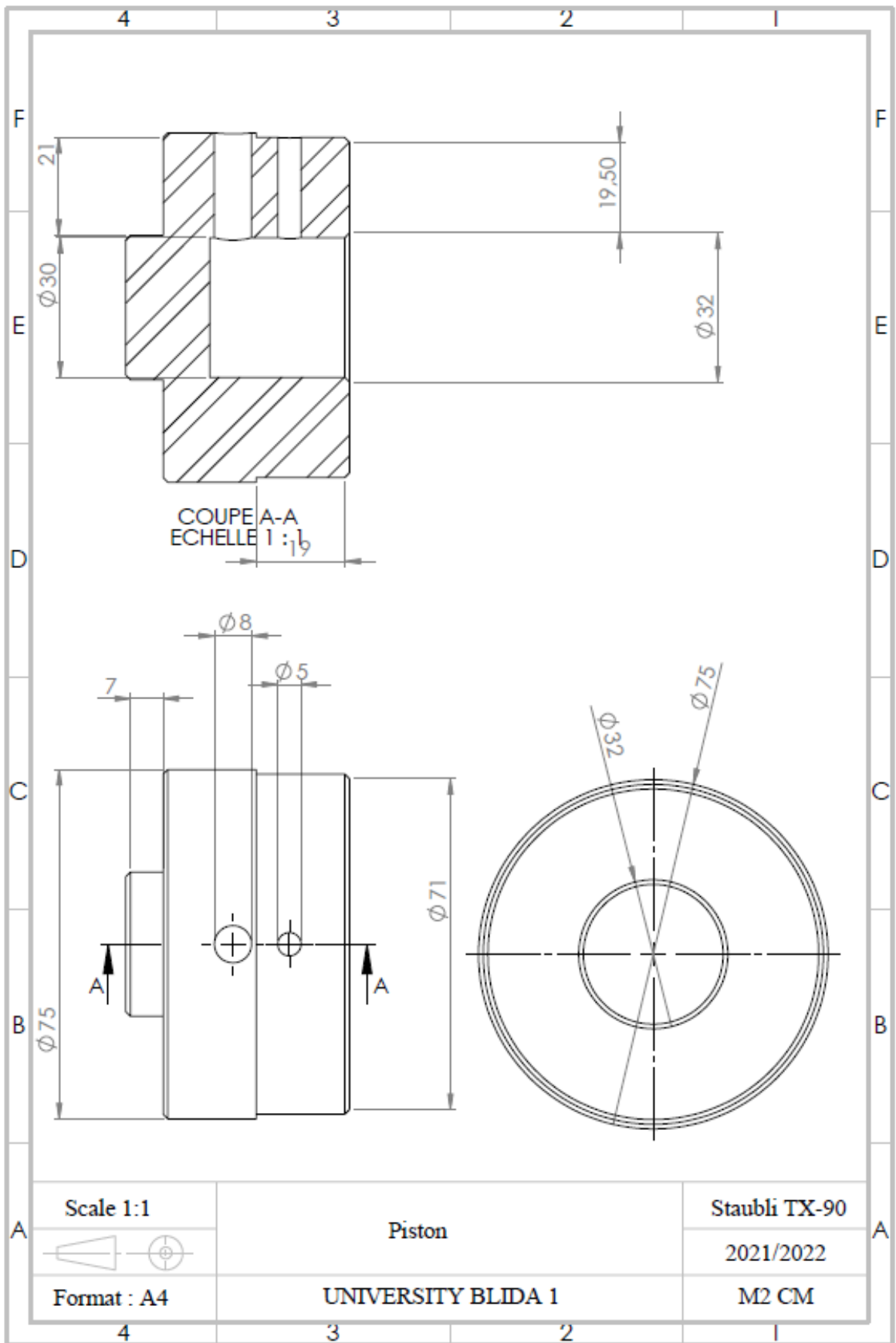


Figure IV.3 The Piston

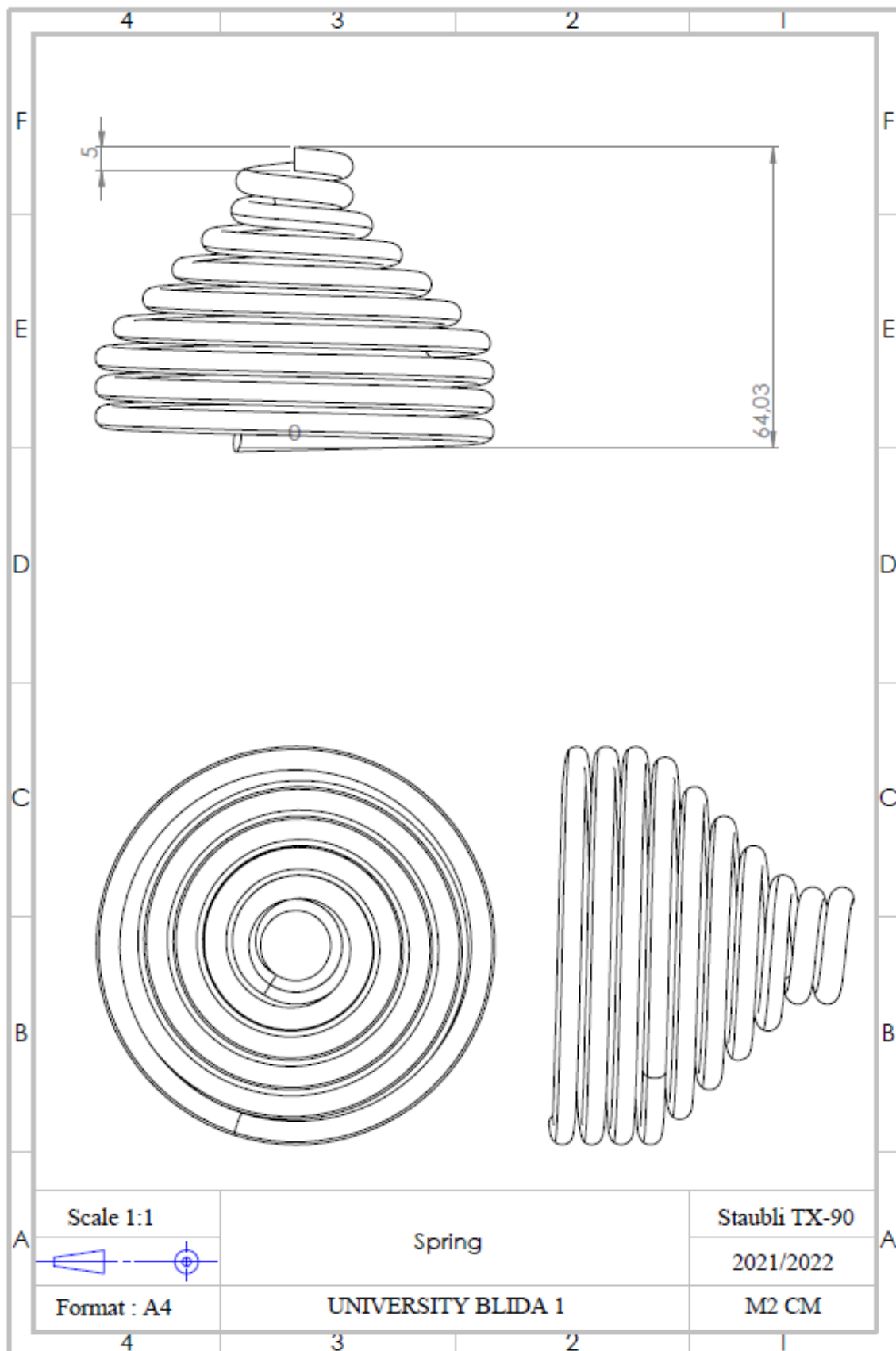


Figure IV.4 The spring

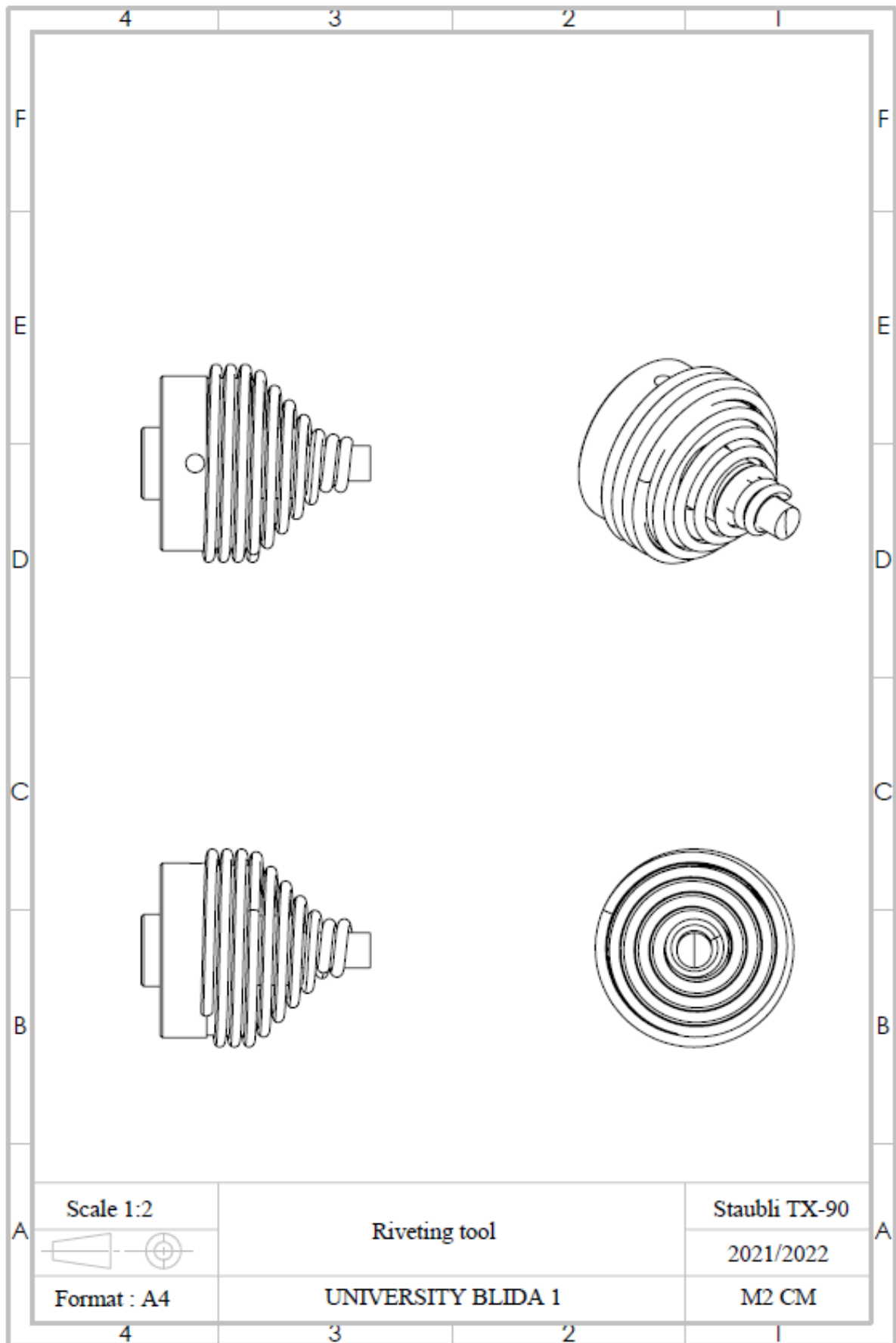


Figure IV.5 Riveting tool

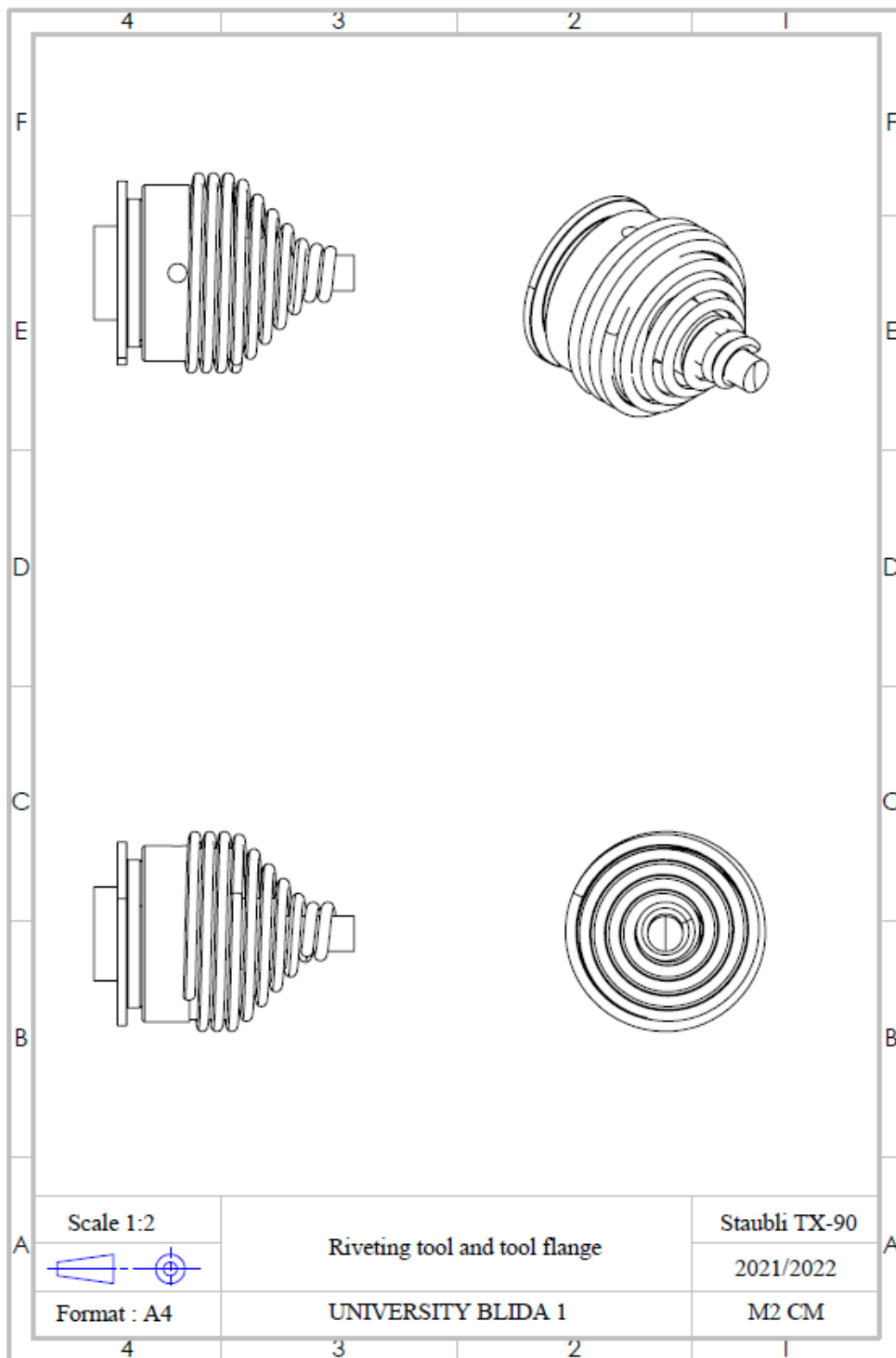


Figure IV.6 Riveting tool and tool flange

IV.4 Inverse dynamics of the system in a free trajectory:

The Staubli TX-90 robot starts from the position “zero” specified by the manufacturer, (all the coordinates have a zero value) towards the executive point. the most unfavorable case that we are going to study is the case where the robot reaches the extreme point, which corresponds to the 4th configuration , after injection of the results of the direct and inverse geometric model, the first order inverse kinematic model and the second order inverse kinematic model in the inverse dynamic model (N-E), we obtained the following results:

Joint positions:

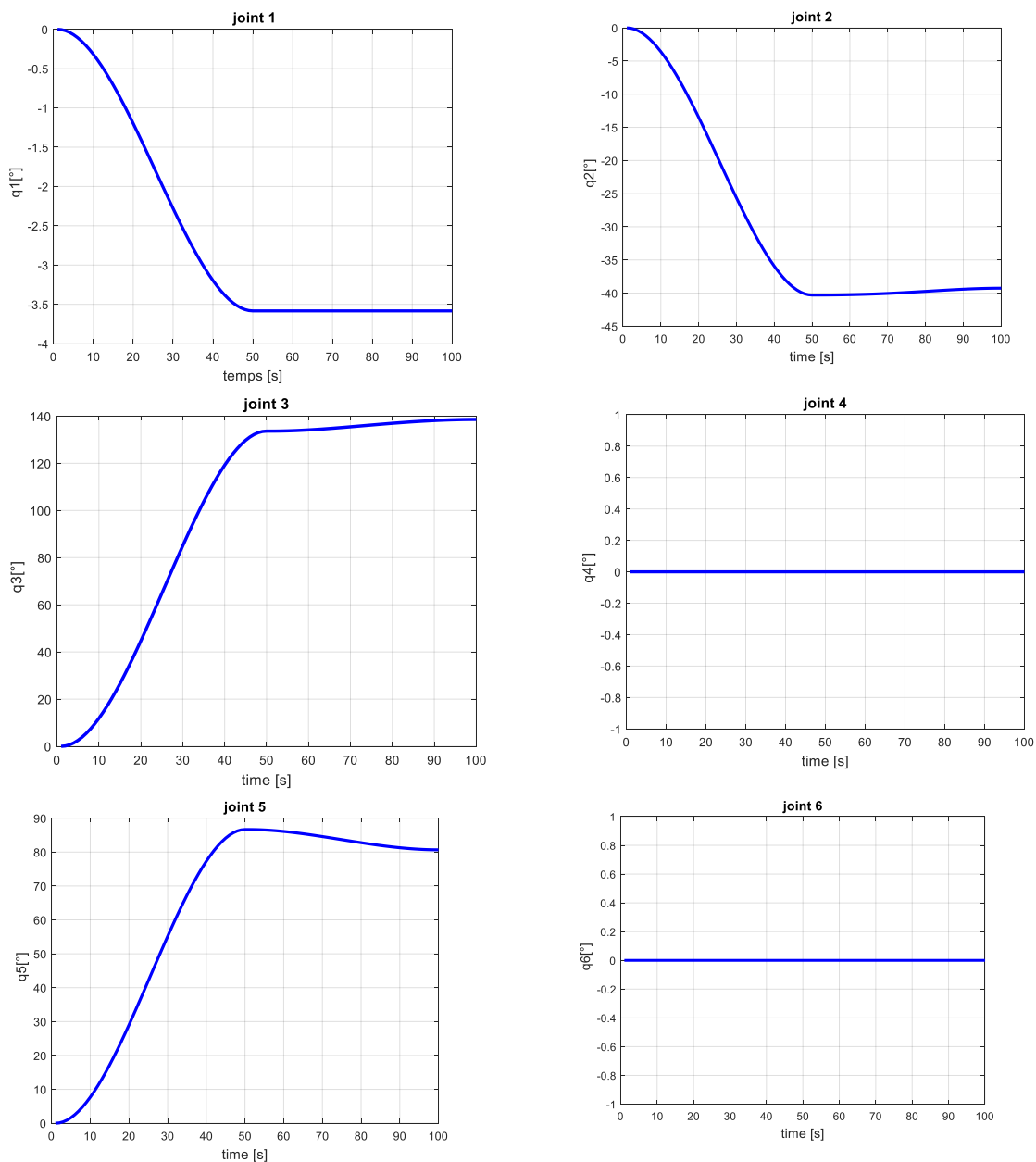


Figure IV.7 Joint positions for Riveting Configuration n°4

Joint velocities :

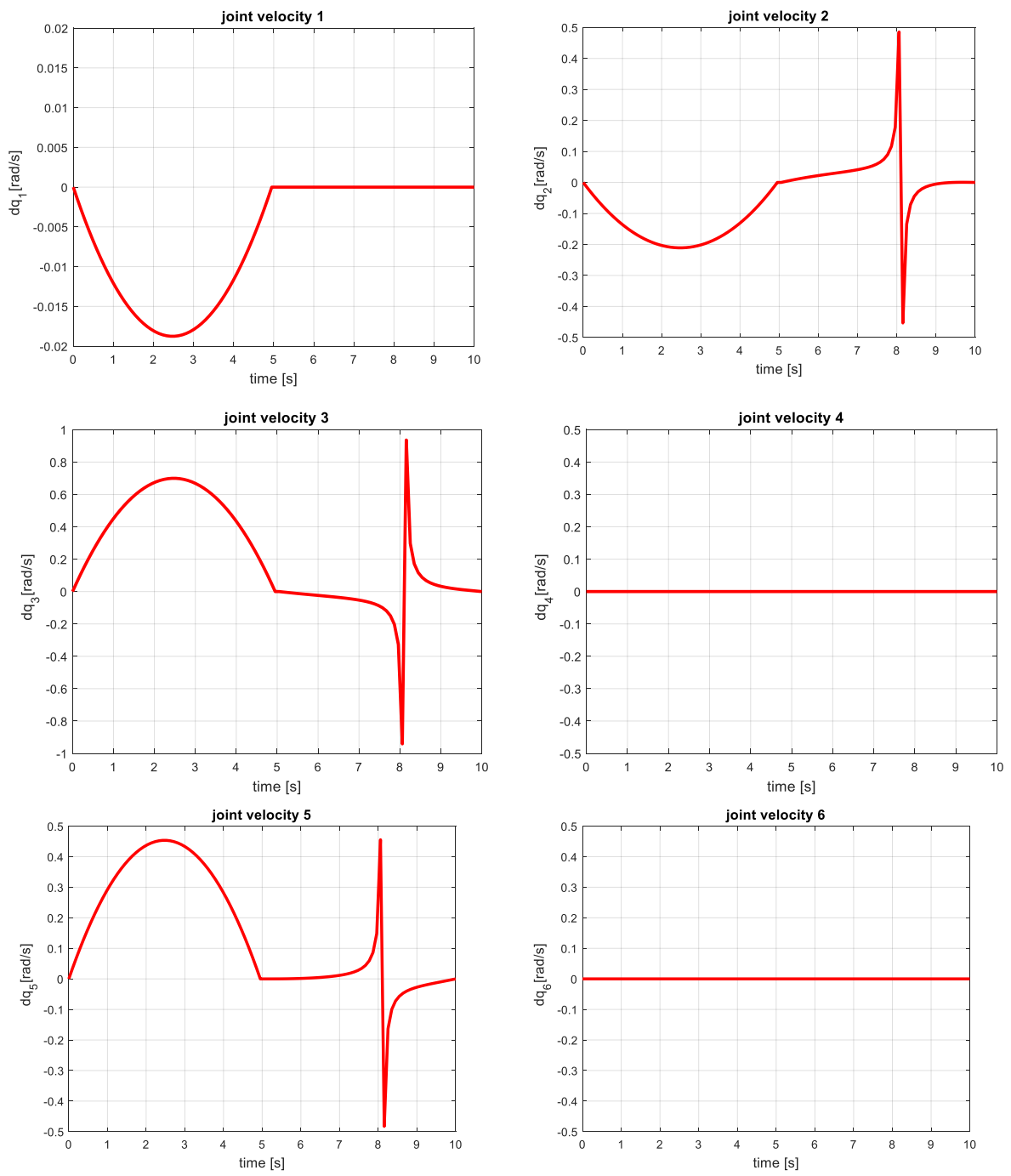


Figure IV.8 Joint velocities for Riveting Configuration n°4

Joint accelerations:

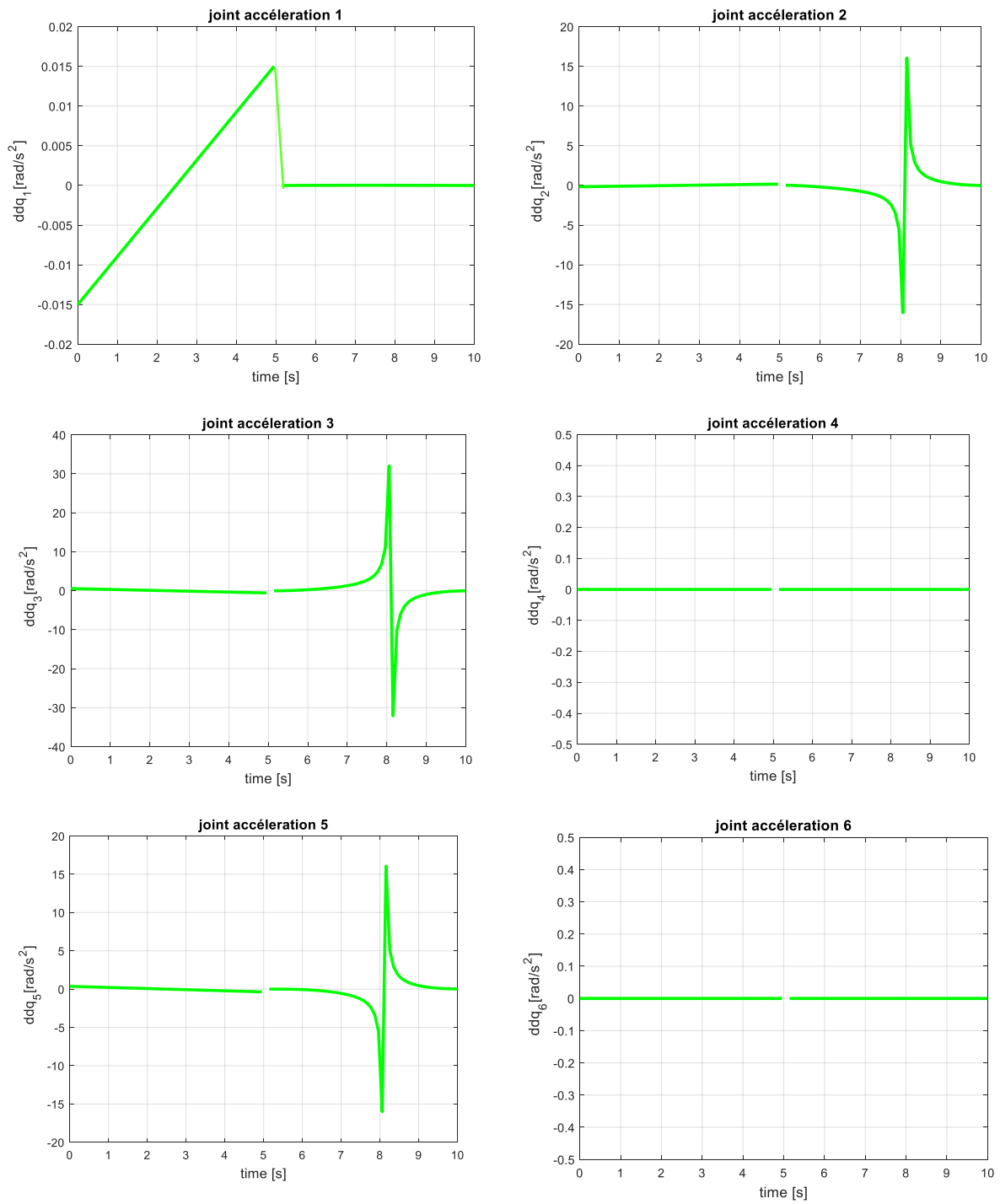


Figure IV.9 joint accelerations for Riveting Configuration n°4

Joint torques :

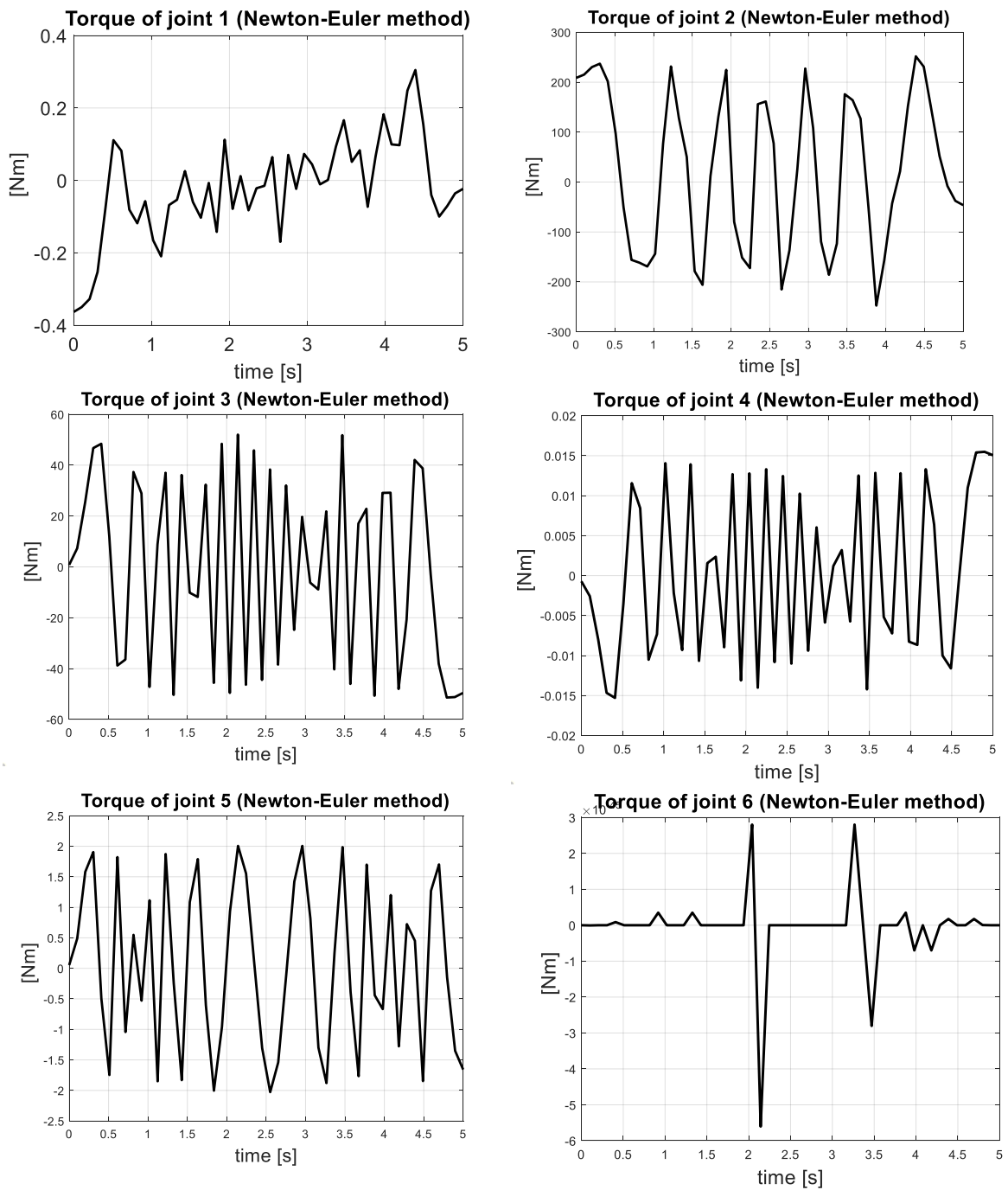


Figure IV.10 Joint torques for Riveting Configuration n°4

Commentary :

Looking at the results in Fig IV.10:

The torques generated by the actuators of the Staubli robot (Fig IV.10) when moving from the position “zero” to the working position are within the tolerance range of the robot , hence ,the robot can perform this task safely.

IV.2 Vibration study using Solidworks software :

In order to verify the vibratory state of the robot, we proceeded to model the satubli tx 90 robot by finite element, using the simulation module installed on Solidworks. We chose 4 configurations (figIV.11, figIV13, figIV15 ,figIV17) , and we got the results (figIV.12 ,figIV.14 ,figIV.16 , figIV.18).

Modal shapes and eigenfrequencies obtained by Solideworks:

1st configuration :

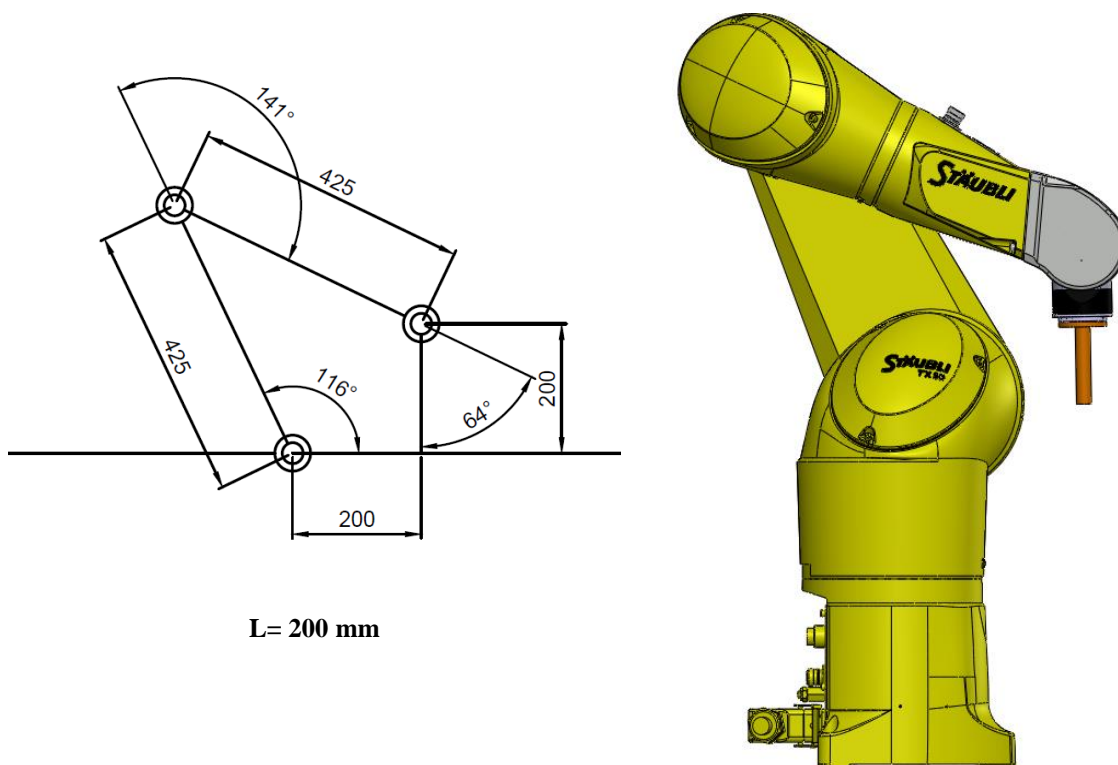
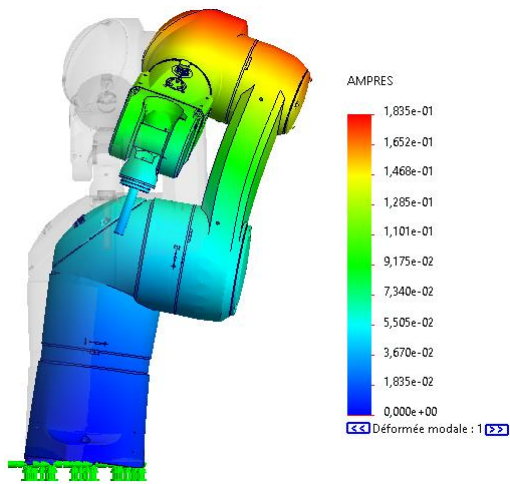
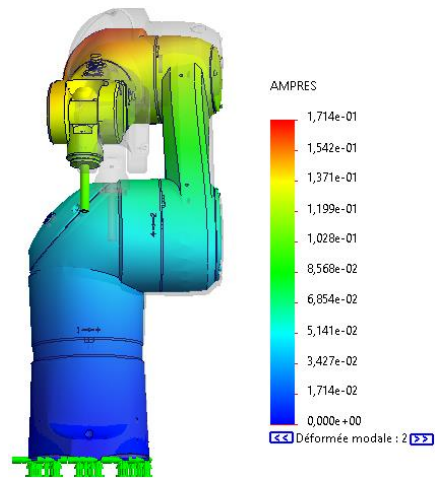


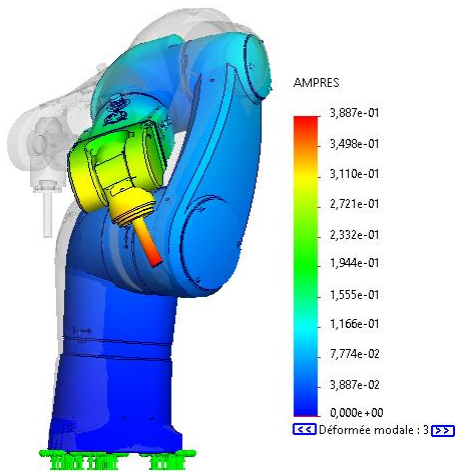
Figure IV.11 1st configuration of the riveting



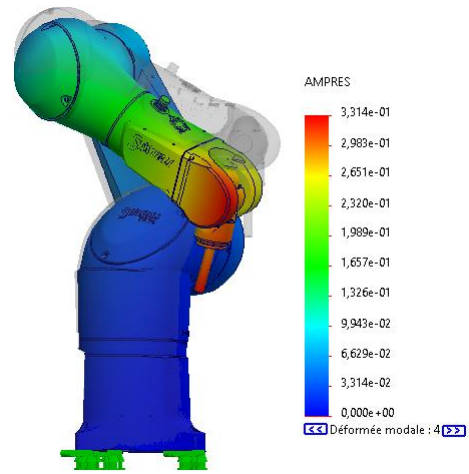
mode1-1flexion $f_p = 105.44$ Hz



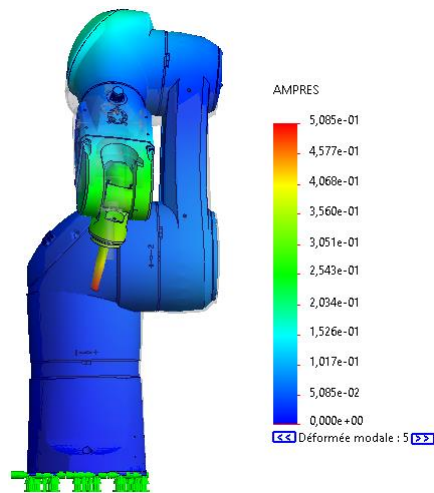
model1-2torsion $f_p = 111.81$ Hz



model1-3torsion $f_p = 182.42$ Hz



model1-4 $f_p = 230.44$ Hz



model1-5torsion $f_p = 345.34$ Hz

Figure IV.12 Modal distortion and natural frequencies of the 1st configuration

2nd configuration :

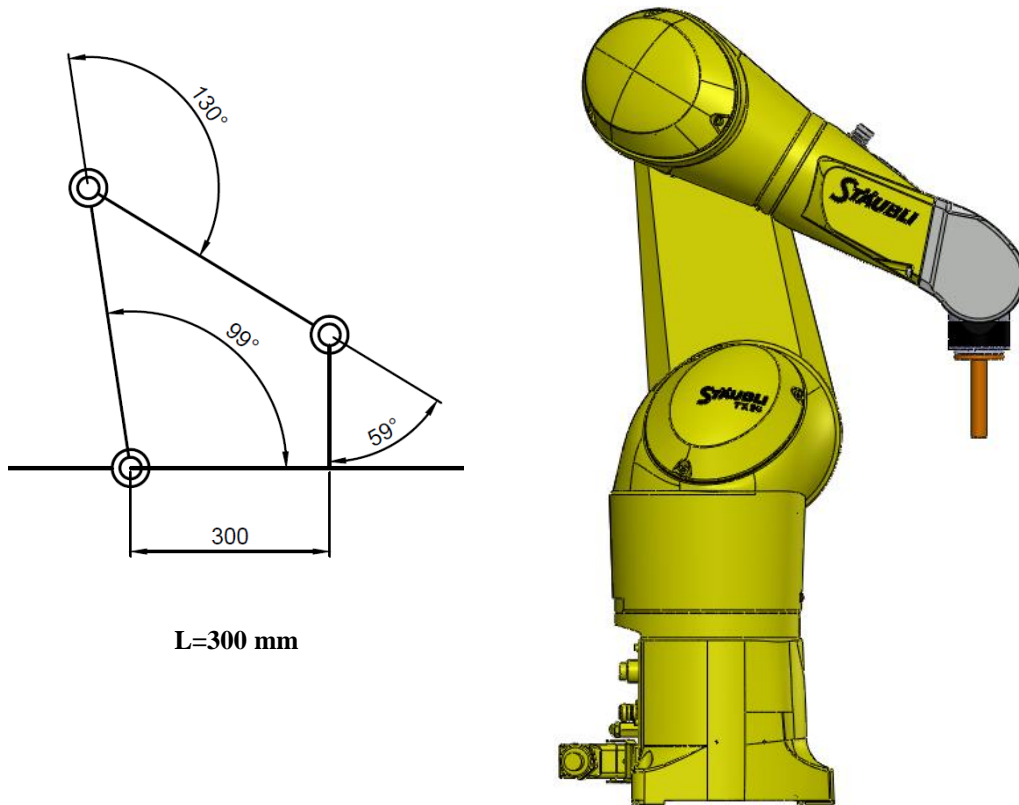
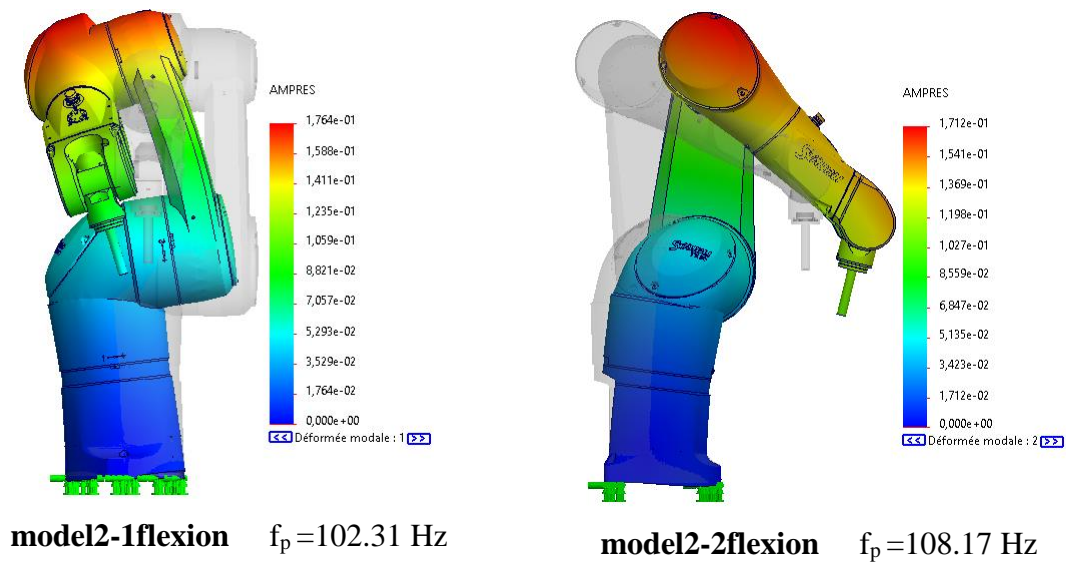
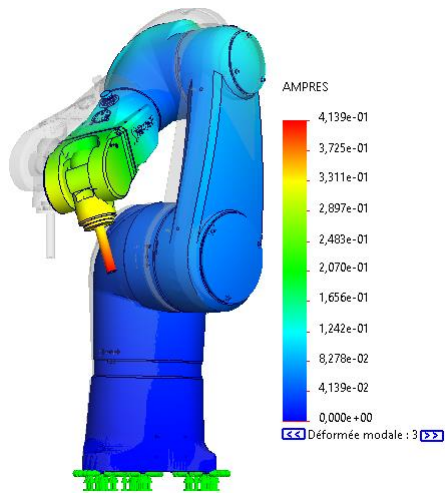
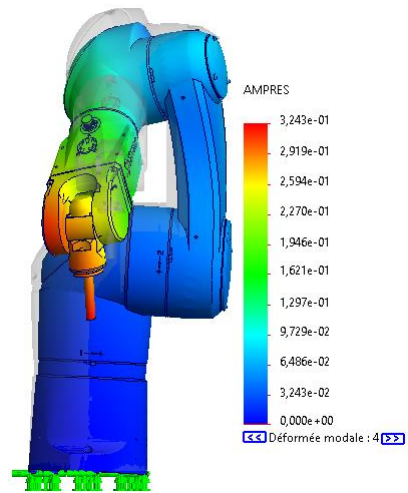


Figure IV.13 2nd configuration of the riveting

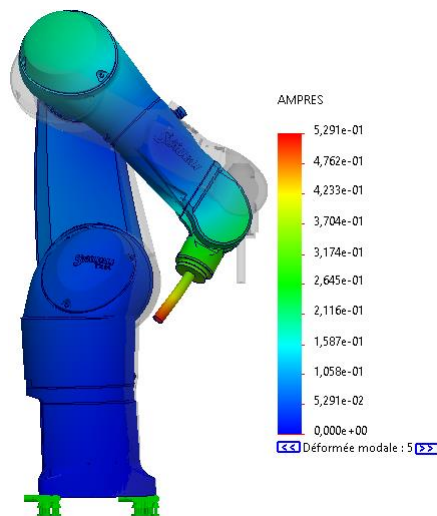




model2-3torsion $f_p = 183.56$ Hz



model2-4torsion $f_p = 220.86$ Hz



model2-5torsion $f_p = 345.5$ Hz

Figure IV.14 Modal distortion and natural frequencies of the 2nd configuration

3rd configuration :

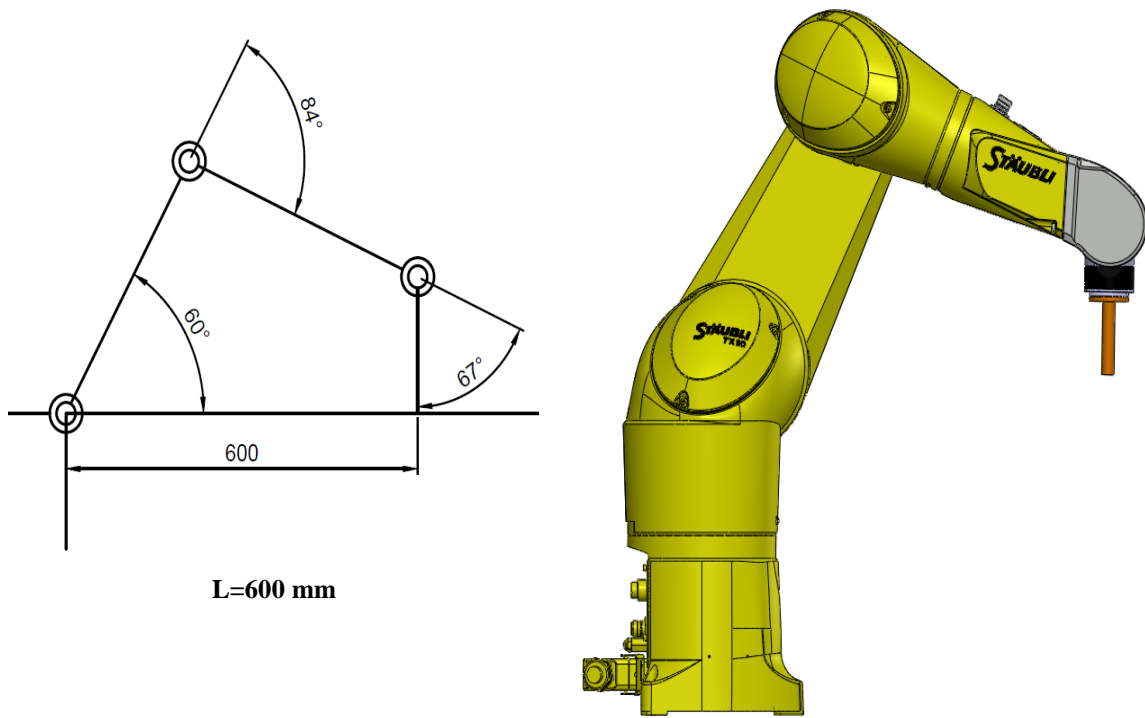
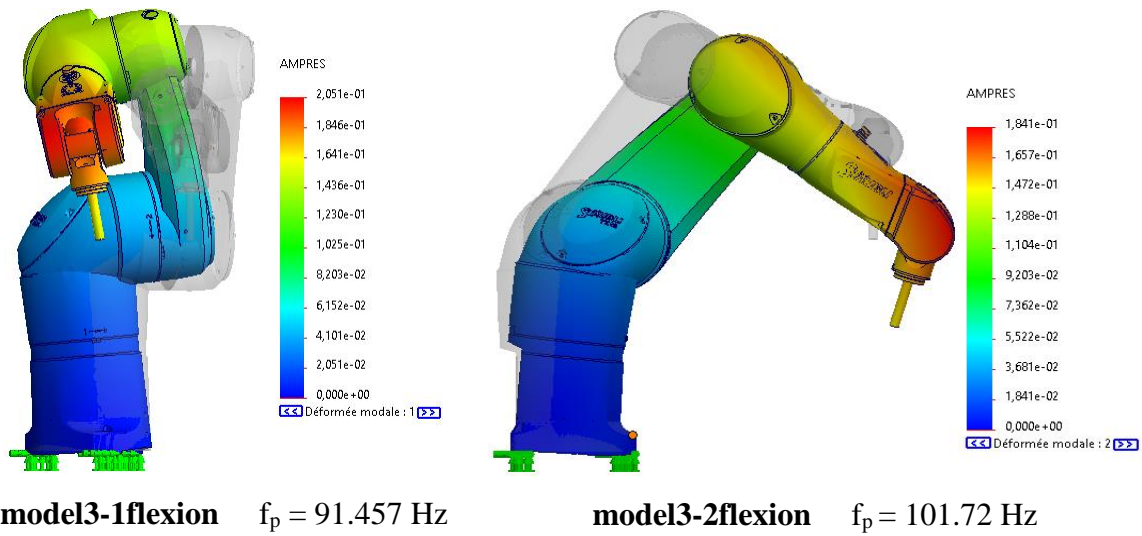
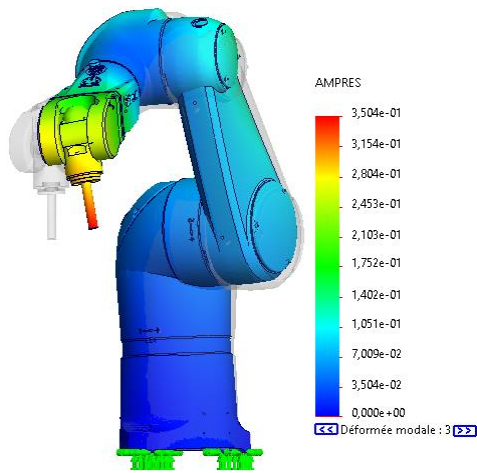
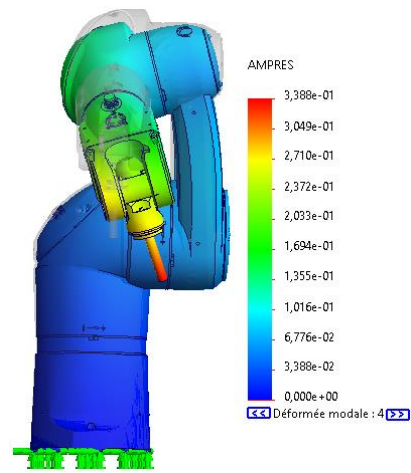


Figure IV.15 3rd configuration of the riveting

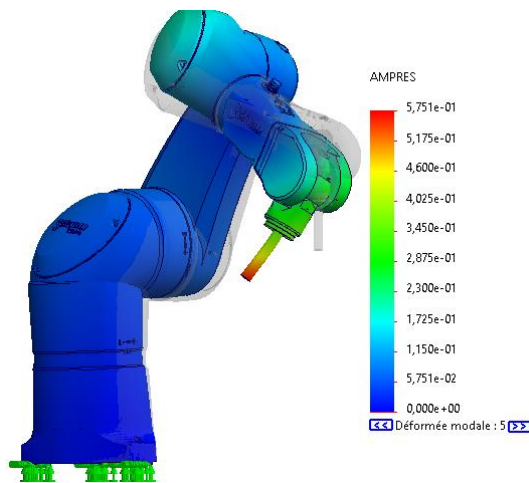




model3-3 $f_p = 183.77$ Hz



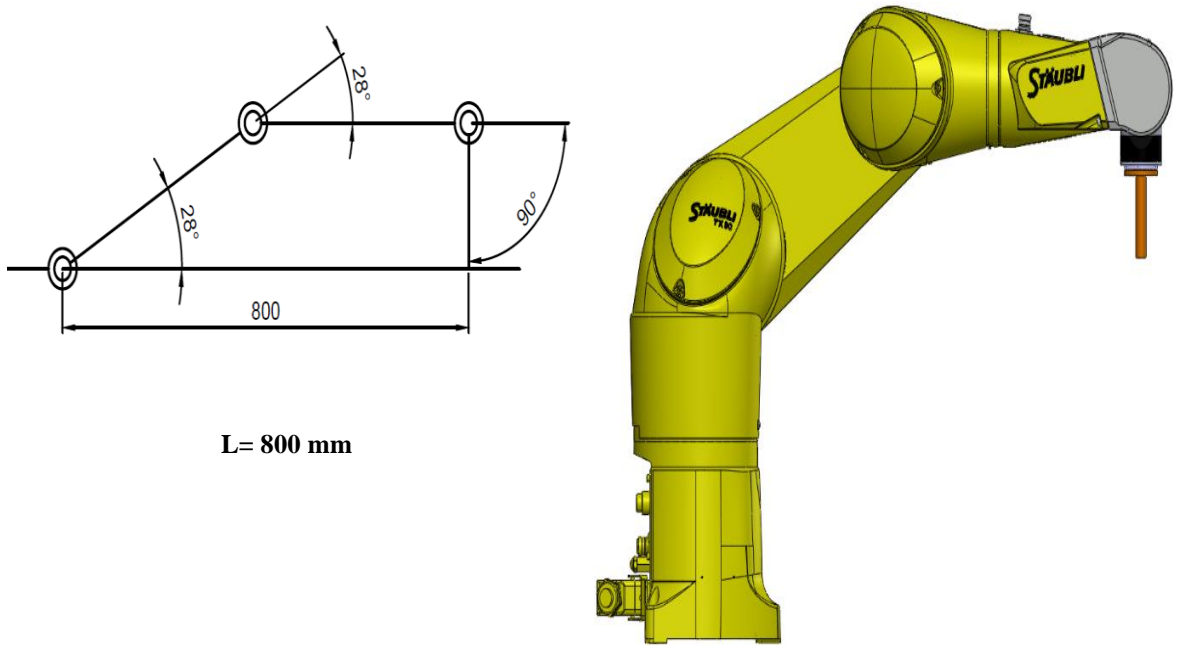
model3-4 $f_p = 206.74$ Hz



model3-5 $f_p = 348.93$ Hz

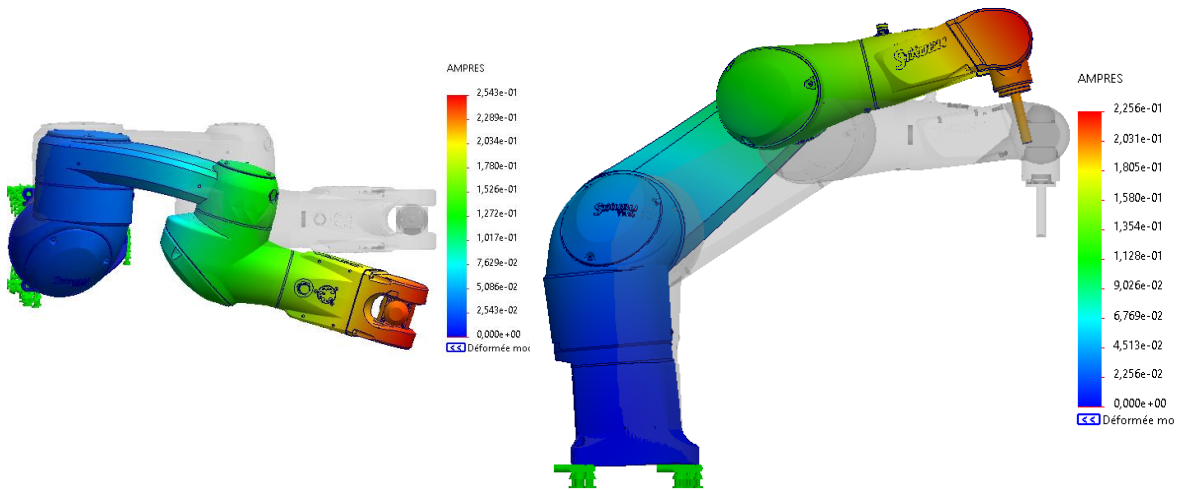
Figure IV.16 Modal distortion and natural frequencies of the 3rd configuration

4th configuration :



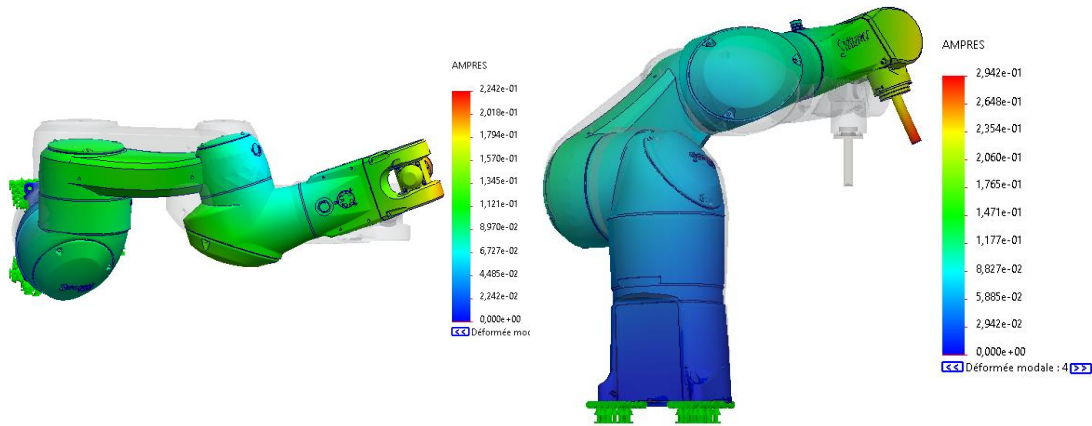
$L = 800 \text{ mm}$

Figure IV.17 4th configuration of the riveting



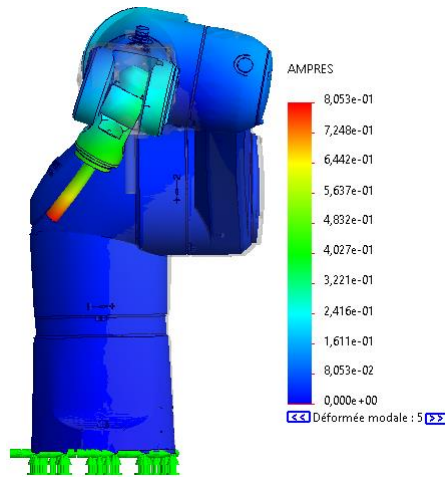
model4-1 $f_p = 81.382 \text{ Hz}$

model4-2 $f_p = 98.362 \text{ Hz}$



model4-4 $f_p = 227.24$ Hz

model4-3 $f_p = 187.26$ Hz



model4-5 $f_p = 414.72$ Hz

Figure IV.18 Modal distortion and natural frequencies of the 4th configuration

Commentary :

The modal calculation of the four configurations obtained by Solidworks allowed us to obtain the first five eigenmodes of each configuration as well as their eigenfrequencies. The analysis of these results allows us to observe:

Configuration1: Figure IV.2 shows the first bending mode of the structure. Its natural frequency is 105.44 Hz. The hammer can generate a sinusoidal force of frequency varies between 10 Hz and 100 Hz depending on the flow of the air entering the hammer and the stiffness of the spring. If the hammer works at a frequency of 100 Hz, the frequency of the excitation force will approach the resonant frequencies of the system from which it is recommended to operate the hammer at a frequency below 80 Hz.

Configuration2: Figure IV.4 shows the first bending mode of the structure. Its natural frequency is 102.31 Hz. The hammer can generate a sinusoidal force of frequency varies between 10 Hz and 100 Hz depending on the flow of the air entering the hammer and the stiffness of the spring. If the hammer works at a frequency of 100 Hz, the frequency of the excitation force will approach the resonant frequencies of the system from which it is recommended to operate the hammer at a frequency below 80 Hz.

Configuration 3: Figure IV.6 shows the first bending mode of the structure. Its natural frequency is 91.457 Hz. The hammer can generate a sinusoidal force of frequency varies between 10 Hz and 100 Hz depending on the flow of the air entering the hammer and the stiffness of the spring. If the hammer works at a frequency of 100 Hz, the frequency of the excitation force will approach the resonant frequencies of the system from which it is recommended to operate the hammer at a frequency below 80 Hz.

Configuration 4: Figure IV.8 shows the first bending mode of the structure. Its natural frequency is 81.382 Hz. The hammer can generate a sinusoidal force of frequency varies between 10 Hz and 100 Hz depending on the flow of the air entering the hammer and the stiffness of the spring. If the hammer works at a frequency of 100 Hz, the frequency of the excitation force approach the resonant frequencies of the second natural mode system, from which it is recommended to operate the hammer at a frequency below 60 Hz.

Conclusion:

To avoid all risks of resonance in all four configurations, it is recommended to operate the hammer at a frequency below 50 HZ.

Generale conclusion

Robotics is proving to be a delicate multidisciplinary field to deal with. Robotic systems find a wide field of application in today's industry.

This modest work makes it possible to introduce oneself to robotics, to apply the concepts of theory acquired and to see some simple applications.

The dynamics of robotic systems is not an easy task. It requires rigorous analytical studies punctuated by various modeling and numerical studies.

The study of the kinematics of the robot, when moving from the zero position to the rivet, is necessary to make the inverse dynamics of the robot, this study allowed us to know that the robot Staubli can perform this task without difficulty.

Newton Euler's recursive algorithm allows the calculation of the MDI in implicit form. It has the advantage of calculating the model in a very short time and it is efficient if it is used in numerical form.

The programs produced are based on the symbolic approach. In this approach, the geometric parameters are replaced by their values, which has allowed us to reduce the execution time of our programs.

A study with Solidworks of the non-damped free system allowed us to calculate the natural frequencies and eigenmode necessary to avoid instability of the system due to the resonance phenomenon.

A blocking of the four and six joints is necessary to avoid having a redundant robot and to reduce the calculation time.

A design of the tool is made to adapt the system to the riveting spot

This work can still be improved and we want it to be followed by other work in the field of robot interaction with the environment such as: machining, polishing, the combination of several trajectories etc.

References :

- [1] Chunlu Li and Shuyong Duan Design and Analysis of Vibration Reduction System to Improve the Track Accuracy of Robot .Arm-Tip Springer Nature Singapore Pte Ltd. 2022.
- [2] Dan Kielsholm Thomsen ,Rune Søre-Knudsen , Ole Balling , Xuping Zhang Vibration control of industrial robot arms by multi-mode time-varying input shaping 2020 Elsevier Ltd. All rights reserved.
- [3] Yaser Mohammadi Keivan Ahmadi Effect of axial vibrations on regenerative chatter in robotic milling 2019 The Authors. Published by Elsevier B.V.
- [4] AOUCHENNI Mourad ,BENMOUSSA Larbi, Master thesis on “Réalisation d’un environnement de modélisation, commande et simulation virtuel des robots manipulateurs ” . Industrial automations ,_University of A. MIRA – BEJAIA 2019/2020.
- [5] Frank Hegel , Claudia Muhl , Britta Wrede , Martina Hielscher-Fastabend , Gerhard Sagerer , Second International Conferences on Advances in Computer-Human Interactions , Understanding Social Robots , Faculty of Technology, Bielefeld University , Germany,2009 .
- [6] BOUMENIR HAMZA & MOUHOUBI RACIM , Master thesis on “Réalisation d’un bras Manipulateur RRR HARMS” , Industrial Automatic and computer science , University of SAAD DAHLAB of BLIDA , 2019-2020.
- [7] Matjaž Mihelj · Tadej Bajd Aleš Ude · Jadran Lenarčič Aleš Stanovnik · Marko Munih Jure Rejc · Sebastjan Šlajpah , Robotics , Second Edition , Library of Congress . 2010) .
- [8] Gumbs AA, De Simone B, Chouillard E. Searching for a better definition of robotic surgery: is it really different from laparoscopy?. *Mini-invasive Surg* 2020;4:90. <http://dx.doi.org/10.20517/2574-1225.2020.110> .
- [9] : SAHIR Kocela ,BOUATMANE Hakim , Master thesis on “ Etude et réalisation d’un bras de robot à base de carte Arduino ” Industrial Automatic and computer science ,University A. MIRA-BEJAIA 25/06/19 .
- [10] (Jean-Louis Boimond ,lecons of “ ROBOTIQUE “., University of Angers).
- [11] MAHER BAILI , Doctorat thesis on “Analyse et classification de manipulateurs 3R à axes orthogonaux ” Mechanical engineering University of Nantes , 13 /12 /2004 .
- [12] ACHERCHOUR Allaoua , ARDJOUNE Nassim Master thesis on “ Commande floue dynamique d’un robot manipulateur ” , Industrial Automatic and computer science , University of Abderrahmane MIRA Bejaia, 2017/2018).
- [13] WISAMA Khalil , Etienne Dombre , Modélisation identification et commande des robots , second edition , HERMES SCIENCE PUBLICATIONS , Paris , 1999.
- [14] Khiair NAIT CHABANE , Doctorat thesis on “Exploitation de la redondance pour la commande coordonnée d’un manipulateur mobile d’assistance aux personnes handicapées ” UNIVERSITY of EVRY – VAL of ESSONNE , Robotic , 30/11 / 2006 .
- [15] BOUZID Abdelbaset & LARBI Allouani , Master thesis on “ETUDE D’UN ROBOT SERIEL” , Mechanical engineering University of M’sila . 2020 / 2021).
- [16] Dr Adnane LABED , lecons of “Technologie de Base ” , Mechanical engineering , University of Mohamed Khider de Biskra , 2014 .
- [17] Dr.AMEUR Toufik , lecons of “ Construction mécanique ” , Mechanical Construction, UNIVERSITY of KASDI MERBAH OUARGLA, 2016-2017.
- [18] Hiba Hage , Doctorat thesis on Identification et simulation physique d’un robot Staubli TX-90 pour le fraisage à grande vitesse. ". Automatic / Robotic. University of Pierre et Marie Curie Paris France , 2012.
- [19] Bruno Siciliano, Oussama Khatib , Springer Handbook of Robotics, 2nd Edition , 2016

[20] Salim Maakaroun , Doctorat thesis on " Modélisation et simulation dynamique d'un véhicule urbain innovant en utilisant le formalisme de la robotique " , Automatic, University of Nantes Angers , 02 /11/2011.

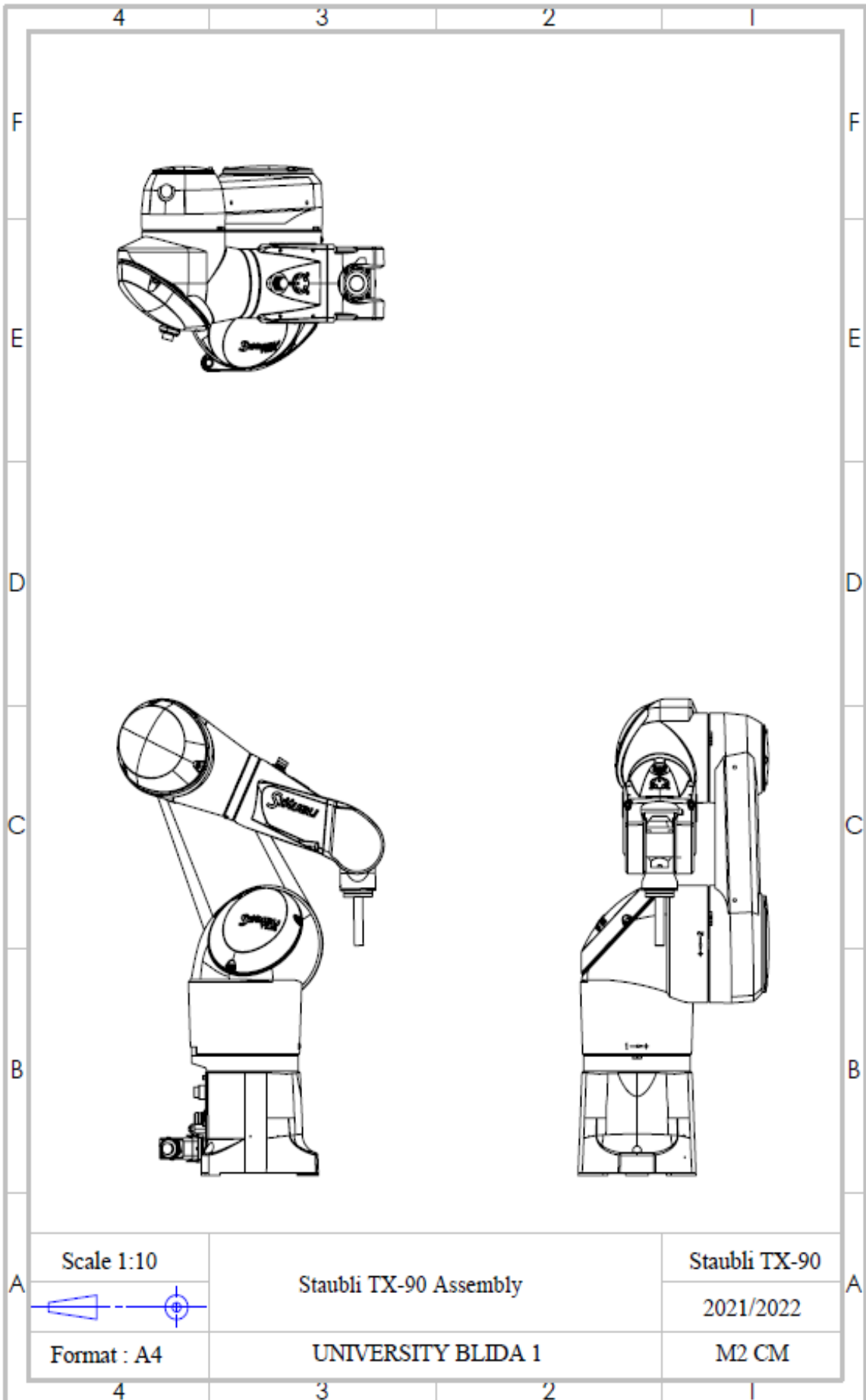
[21] S.Rajasekaran , Structural dynamics of earthquake engineering , theory and application using MATHEMATICA and MATLAB , edition crc press , 2009.

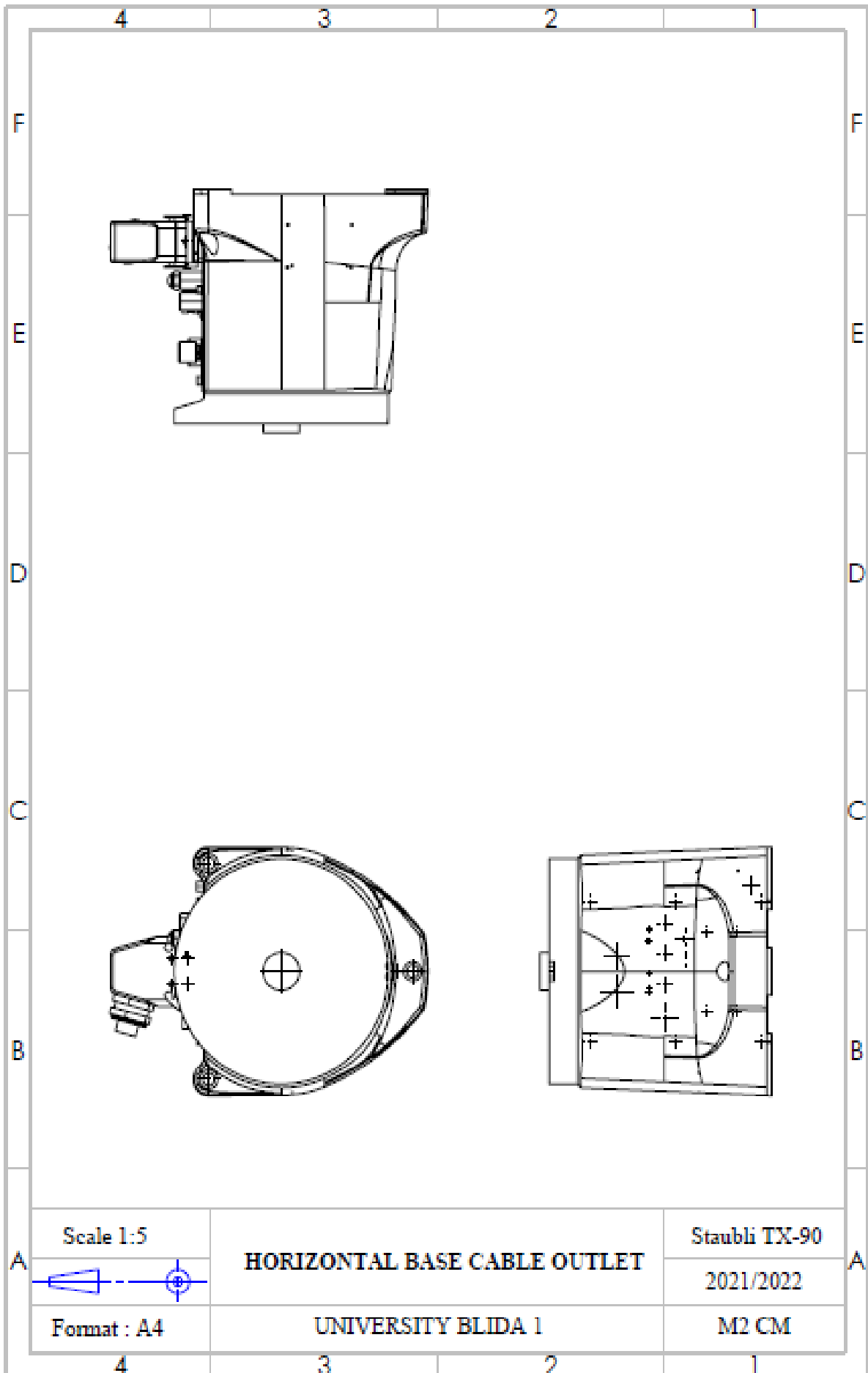
[22] Ronghui Zheng, Siyu Ren, Guoping Chen, Huaihai Chen , Multi-shaker half sine shock on random mixed vibration control Available online 28 July 2021journal homepage: www.elsevier.com/locate/jsvi.

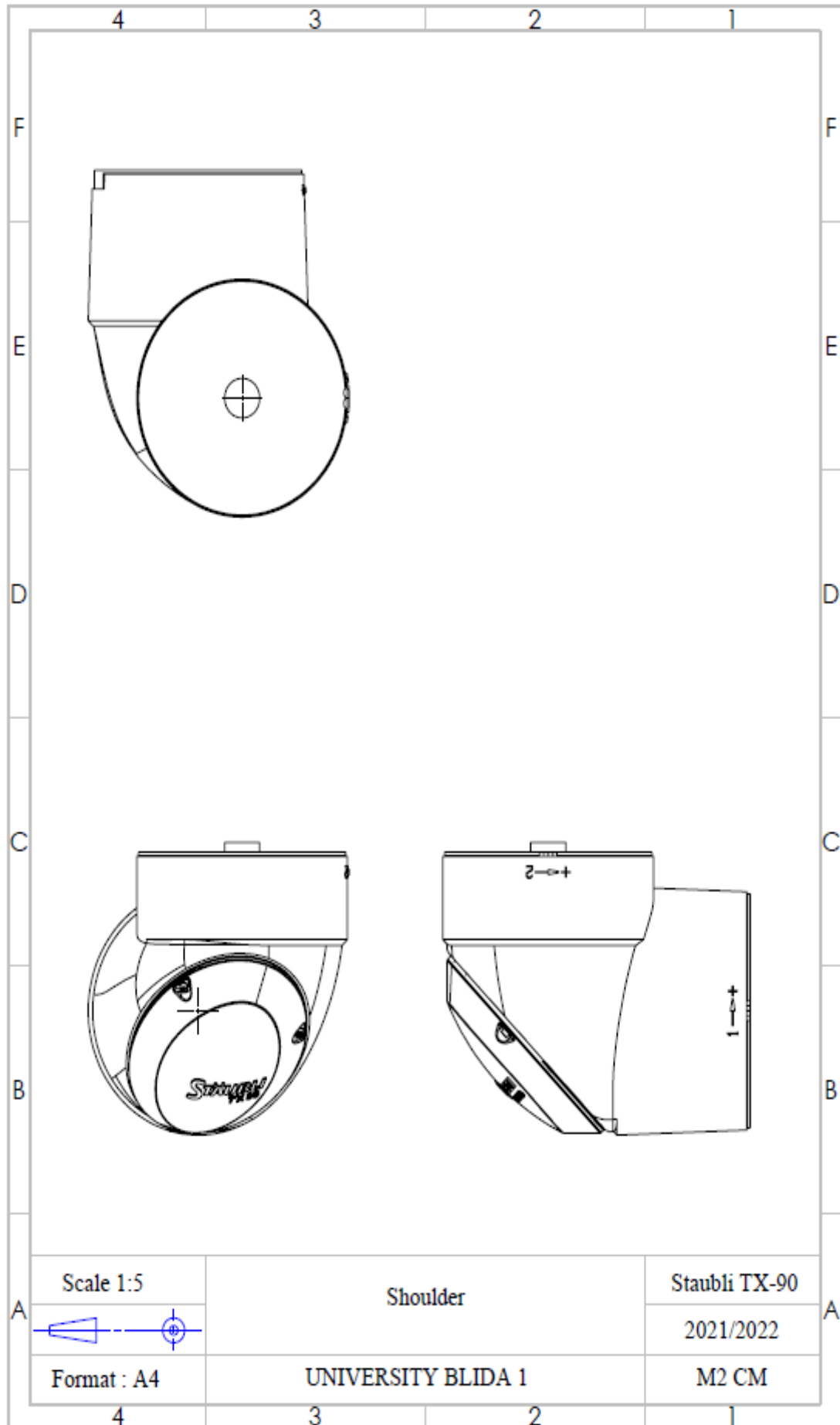
[23] Feng-Feng Xi .Lin Yu.Xiao-wei Tu .Framework on robotic percussive riveting for aircraft assembly automation . springer 2013 .

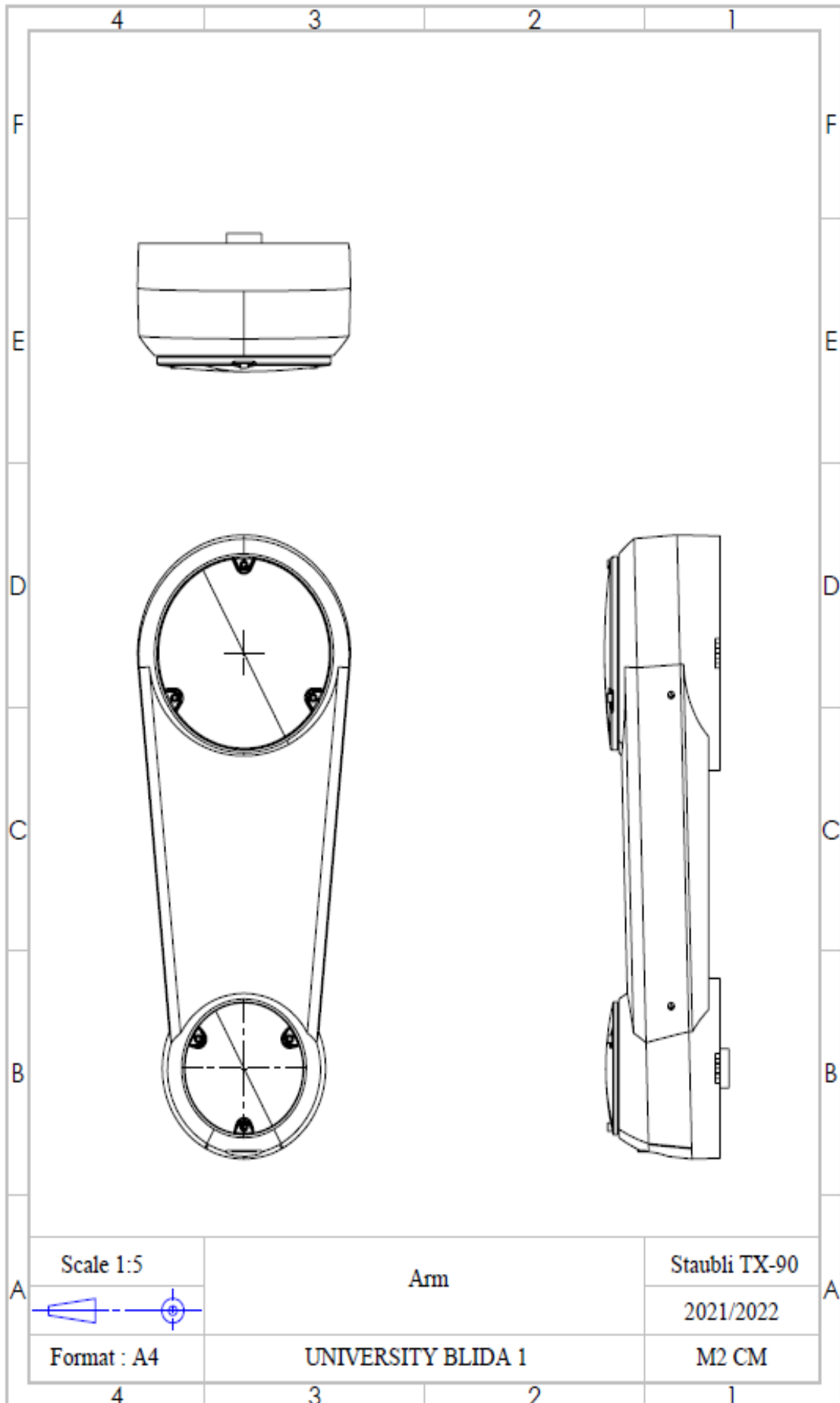
Appendix A

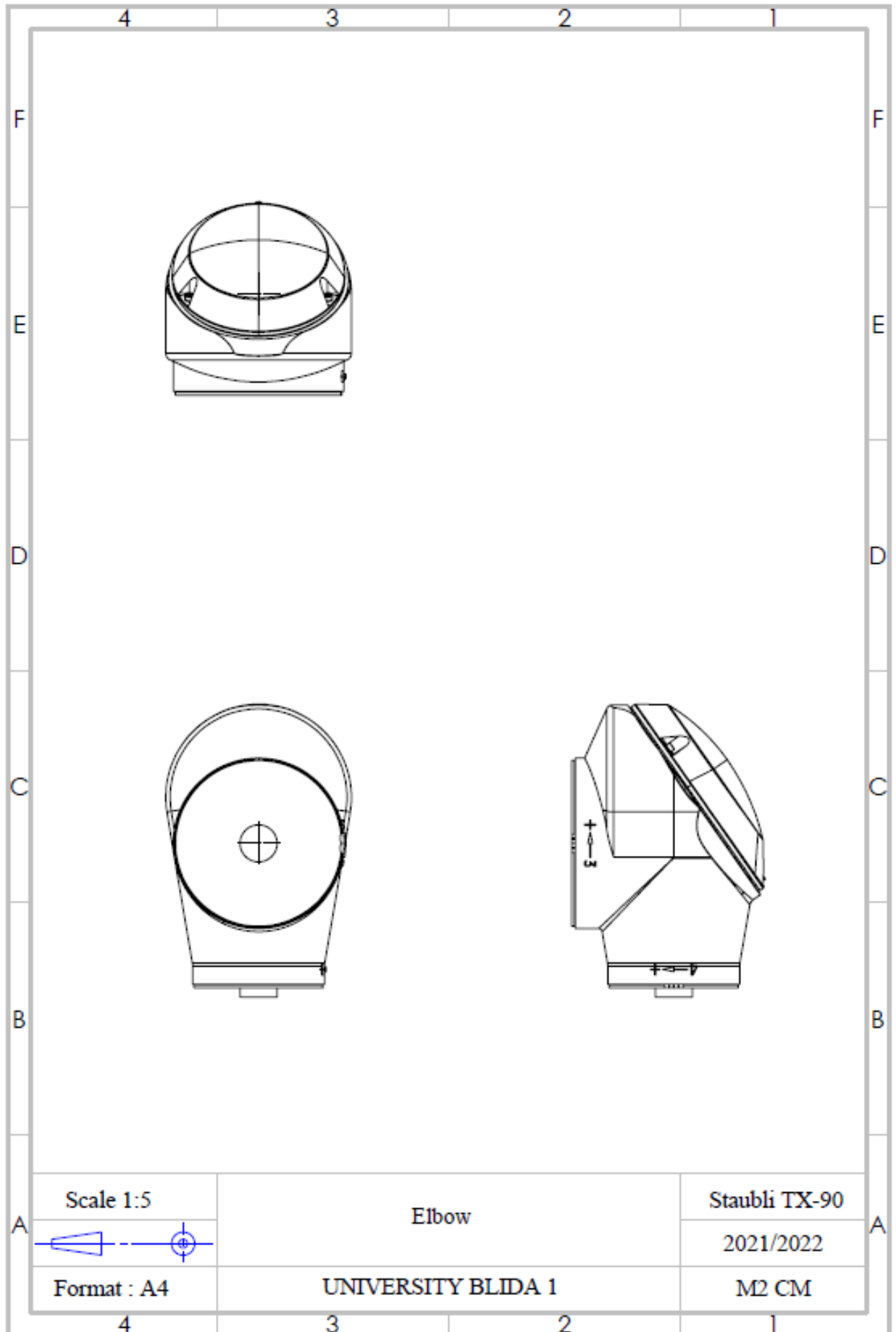
2D DRAWING OF Staubli robot

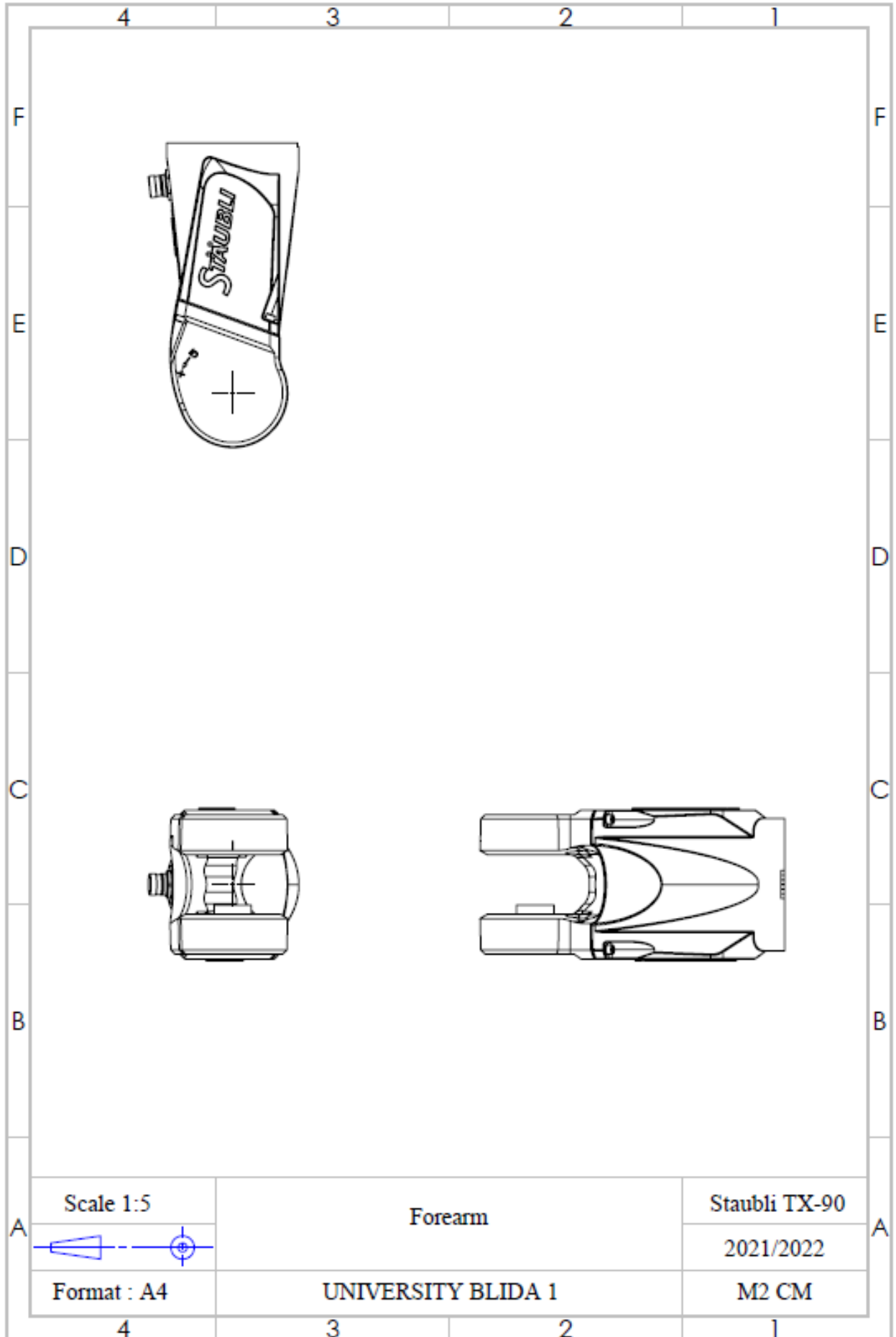








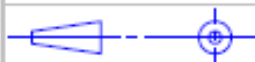




Scale 1:5

Forearm

Staubli TX-90

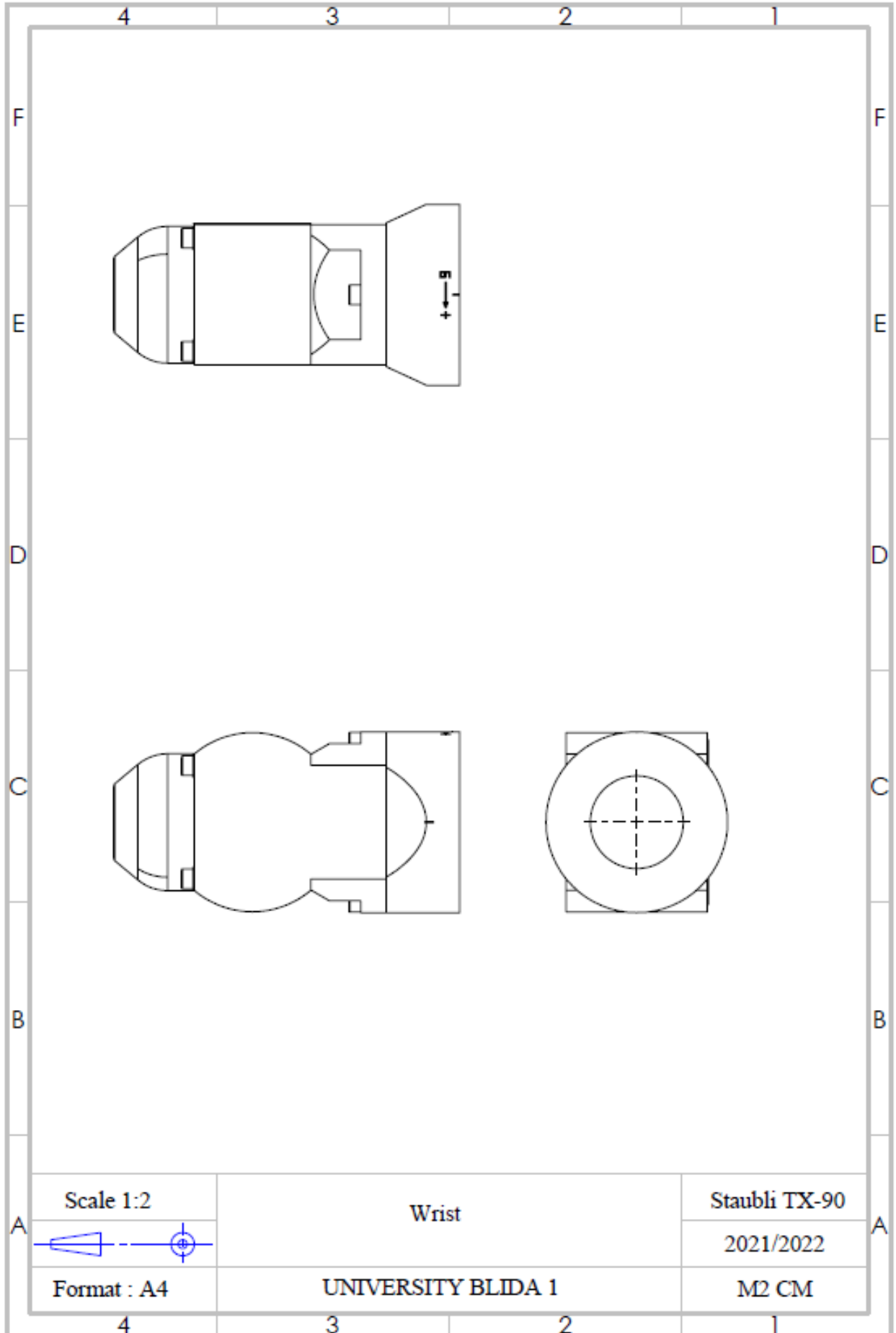


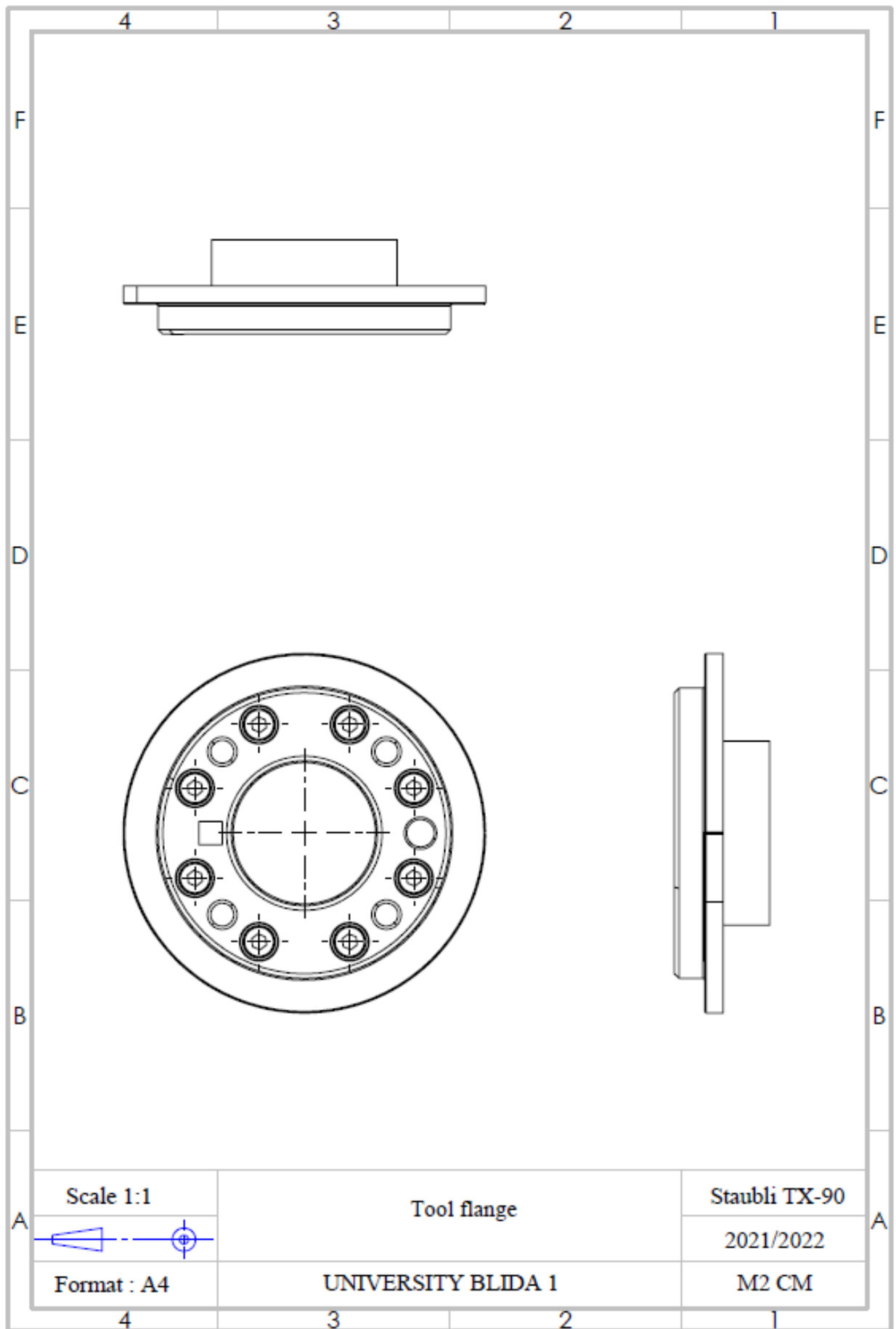
2021/2022

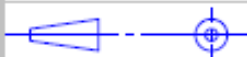
Format : A4

UNIVERSITY BLIDA 1

M2 CM





Scale 1:1

 Format : A4

Tool flange
 UNIVERSITY BLIDA 1

Staubli TX-90
 2021/2022
 M2 CM

Appendix B

Mass properties of STAUBLI TX90

1/Mass properties of TX90 SHOULDER

Configuration: Default

Coordinate system: R1

Mass = 45.722 kilograms

Volume = 0.017 cubic meters

Surface area = 0.377 square meters

Center of mass (meters)

X = 0.019

Y = 0.025

Z = -0.064

Principal axes of inertia and principal moments of inertia : (kilograms *square meters)

Taken at the center of mass .

Ix = (0.306, 0.424, 0.852) Px = 0.359

Iy = (-0.396, -0.758, 0.519) Py = 0.599

Iz = (0.866, -0.496, -0.064) Pz = 0.630

Moments of inertia : (kilograms *square meters)

Taken at the center of mass and aligned with the output coordinate system .

Lxx = 0.600 Lxy = 0.045 Lxz = 0.064

Lyx = 0.045 Lyy = 0.563 Lyz = 0.086

Lzx = 0.064 Lzy = 0.086 Lzz = 0.425

Moments of inertia : (kilograms *square meters)

Taken at the output coordinate system.

Ixx = 0.818 Ixy = 0.067 Ixz = 0.008

Iyx = 0.067 Iyy = 0.770 Iyz = 0.012

Izx = 0.008 Izy = 0.012 Izz = 0.470

2/Mass properties of **TX90 ARM**

Configuration: Default

Coordinate system: R2

Mass = 35.066kilograms

Volume = 0.013cubic meters

Surface area = 0.400square meters

Center of mass (meters)

X = 0.173

Y = 0.000

Z = 0.221

Principal axes of inertia and principal moments of inertia : (kilograms *square meters)

Taken at the center of mass .

I_x = (-1.000, 0.000, 0.008) P_x = 0.147

I_y = (0.000, -1.000, 0.000) P_y = 1.149

I_z = (0.008, 0.000, 1.000) P_z = 1.222

Moments of inertia : (kilograms *square meters)

Taken at the center of mass and aligned with the output coordinate system .

L_{xx} = 0.147 L_{xy} = 0.000 L_{xz} = -0.009

L_{yx} = 0.000 L_{yy} = 1.149 L_{yz} = 0.000

L_{zx} = -0.009 L_{zy} = 0.000 L_{zz} = 1.222

Moments of inertia : (kilograms *square meters)

Taken at the output coordinate system.

I_{xx} = 1.863 I_{xy} = 0.000 I_{xz} = 1.337

I_{yx} = 0.000 I_{yy} = 3.920 I_{yz} = 0.000

I_{zx} = 1.337 I_{zy} = 0.000 I_{zz} = 2.277

3/Mass properties of **TX90 ELBOW**

Configuration: Default

Coordinate system: R3

Mass = 20.254kilograms

Volume = 0.008cubic meters

Surface area = 0.220square meters

Center of mass (meters)

X = 0.000

Y = -0.004

Z = 0.015

Principal axes of inertia and principal moments of inertia : (kilograms *square meters)

Taken at the center of mass .

Ix = (0.000, 0.988, 0.155) Px = 0.091

Iy = (0.000, -0.155, 0.988) Py = 0.156

Iz = (1.000, 0.000, 0.000) Pz = 0.160

Moments of inertia : (kilograms *square meters)

Taken at the center of mass and aligned with the output coordinate system .

Lxx = 0.160 Lxy = 0.000 Lxz = 0.000

Lyx = 0.000 Lyy = 0.092 Lyz = 0.010

Lzx = 0.000 Lzy = 0.010 Lzz = 0.154

Moments of inertia : (kilograms *square meters)

Taken at the output coordinate system.

Ixx = 0.164 Ixy = 0.000 Ixz = 0.000

Iyx = 0.000 Iyy = 0.097 Iyz = 0.009

Izx = 0.000 Izy = 0.009 Izz = 0.155

4/ Mass properties of **TX90 FOREARAM**

Configuration: Default

Coordinate system: R4

Mass = 12.258kilograms

Volume = 0.005cubic meters

Surface area = 0.218square meters

Center of mass (meters)

X = -0.002

Y = 0.000

Z = -0.128

Principal axes of inertia and principal moments of inertia : (kilograms *square meters)

Taken at the center of mass .

Ix = (-0.023, -0.002, 1.000) Px = 0.039

Iy = (0.000, -1.000, -0.002) Py = 0.104

Iz = (1.000, 0.000, 0.023) Pz = 0.117

Moments of inertia : (kilograms *square meters)

Taken at the center of mass and aligned with the output coordinate system .

Lxx = 0.117 Lxy = 0.000 Lxz = -0.002

Lyx = 0.000 Lyy = 0.104 Lyz = 0.000

Lzx = -0.002 Lzy = 0.000 Lzz = 0.039

Moments of inertia : (kilograms *square meters)

Taken at the output coordinate system.

Ixx = 0.318 Ixy = 0.000 Ixz = 0.002

Iyx = 0.000 Iyy = 0.305 Iyz = 0.000

Izx = 0.002 Izy = 0.000 Izz = 0.039

5/Mass properties of **TX90 WRIST**

Configuration: Default

Coordinate system: R5

Mass = 1.468kilograms

Volume = 0.001cubic meters

Surface area = 0.047square meters

Center of mass (meters)

X = 0.000

Y = -0.022

Z = 0.001

Principal axes of inertia and principal moments of inertia : (kilograms *square meters)

Taken at the center of mass .

Ix = (0.000, -1.000, -0.009) Px = 0.001

Iy = (1.000, 0.000, 0.000) Py = 0.003

Iz = (0.000, -0.009, 1.000) Pz = 0.003

Moments of inertia : (kilograms *square meters)

Taken at the center of mass and aligned with the output coordinate system .

Lxx = 0.003 Lxy = 0.000 Lxz = 0.000

Lyx = 0.000 Lyy = 0.001 Lyz = 0.000

Lzx = 0.000 Lzy = 0.000 Lzz = 0.003

Moments of inertia : (kilograms *square meters)

Taken at the output coordinate system.

Ixx = 0.003 Ixy = 0.000 Ixz = 0.000

Iyx = 0.000 Iyy = 0.001 Iyz = 0.000

Izx = 0.000 Izy = 0.000 Izz = 0.004

6/Mass properties of **TX90 TOOL FLANGE**

Configuration: Default

Cordinate system: R6

Mass = 0.117kilograms

Volume = 0.000cubic meters

Surface area = 0.016square meters

Center of mass (meters)

X = 0.000

Y = 0.000

Z = 0.091

Principal axes of inertia and principal moments of inertia : (kilograms *square meters)

Taken at the center of mass .

Ix = (-0.003, 1.000, 0.000) Px = 0.000

Iy = (-1.000, -0.003, 0.001) Py = 0.000

Iz = (0.001, 0.000, 1.000) Pz = 0.000

Moments of inertia : (kilograms *square meters)

Taken at the center of mass and aligned with the output coordinate system .

Lxx = 0.000 Lxy = 0.000 Lxz = 0.000

Lyx = 0.000 Lyy = 0.000 Lyz = 0.000

Lzx = 0.000 Lzy = 0.000 Lzz = 0.000

Moments of inertia : (kilograms *square meters)

Taken at the output coordinate system.

Ixx = 0.001 Ixy = 0.000 Ixz = 0.000

Iyx = 0.000 Iyy = 0.001 Iyz = 0.000

Izx = 0.000 Izy = 0.000 Izz = 0.000

7/Mass properties of **TX90 Piston**

Configuration: Default

Coordinate system: Default

Mass = 1.24kilograms

Volume = 0.000cubic meters

Surface area = 0.02square meters

Center of mass (meters)

X = -0.03

Y = 0.00

Z = 0.07

Principal axes of inertia and principal moments of inertia : (kilograms *square meters)

Taken at the center of mass .

$I_x = (0.00, 0.00, 1.00)$ $P_x = 0.00$

$I_y = (0.00, -1.00, 0.00)$ $P_y = 0.00$

$I_z = (1.00, 0.00, 0.00)$ $P_z = 0.00$

Moments of inertia : (kilograms *square meters)

Taken at the center of mass and aligned with the output coordinate system .

$L_{xx} = 0.000$ $L_{xy} = 0.000$ $L_{xz} = 0.000$

$L_{yx} = 0.000$ $L_{yy} = 0.000$ $L_{yz} = 0.000$

$L_{zx} = 0.000$ $L_{zy} = 0.000$ $L_{zz} = 0.000$

Moments of inertia : (kilograms *square meters)

Taken at the output coordinate system.

$I_{xx} = 0.001$ $I_{xy} = 0.000$ $I_{xz} = 0.000$

$I_{yx} = 0.000$ $I_{yy} = 0.001$ $I_{yz} = 0.000$

$I_{zx} = 0.000$ $I_{zy} = 0.000$ $I_{zz} = 0.000$

8/Mass properties of **TX90 Cylinder**

Configuration: Default

Coordinate system: Default

Mass = 0.32kilograms

Volume = 0.000cubic meters

Surface area = 0.01square meters

Center of mass (meters)

X = -0.07

Y = 0.00

Z = 0.17

Principal axes of inertia and principal moments of inertia : (kilograms *square meters)

Taken at the center of mass .

Ix = (1.00, 0.00, 0.00) Px = 0.00

Iy = (0.00, 0.00, -1.00) Py = 0.00

Iz = (0.00, 1.00, 0.00) Pz = 0.00

Moments of inertia : (kilograms *square meters)

Taken at the center of mass and aligned with the output coordinate system .

Lxx = 0.00 Lxy = 0.00 Lxz = 0.00

Lyx = 0.00 Lyy = 0.00 Lyz = 0.00

Lzx = 0.00 Lzy = 0.00 Lzz = 0.00

Moments of inertia : (kilograms *square meters)

Taken at the output coordinate system.

Ixx = 0.01 Ixy = 0.00 Ixz = 0.00

Iyx = 0.00 Iyy = 0.01 Iyz = 0.00

Izx = 0.00 Izy = 0.00 Izz = 0.00

9/Mass properties of **TX90 Spring**

Configuration: Default

Coordinate system: Default

Mass = 0.26kilograms

Volume = 0.000cubic meters

Surface area = 0.03square meters

Center of mass (meters)

X = 0.07

Y = 0.09

Z = 0.06

Principal axes of inertia and principal moments of inertia : (kilograms *square meters)

Taken at the center of mass .

Ix = (-0.46, 0.89, -0.04) Px = 0.00

Iy = (-0.89, -0.46, -0.04) Py = 0.00

Iz = (-0.05, 0.02, 1.00) Pz = 0.00

Moments of inertia : (kilograms *square meters)

Taken at the center of mass and aligned with the output coordinate system .

Lxx = 0.00 Lxy = 0.00 Lxz = 0.00

Lyx = 0.00 Lyy = 0.00 Lyz = 0.00

Lzx = 0.00 Lzy = 0.00 Lzz = 0.00

Moments of inertia : (kilograms *square meters)

Taken at the output coordinate system.

Ixx = 0.00 Ixy = 0.00 Izx = 0.00

Iyx = 0.00 Iyy = 0.00 Iyz = 0.00

Izx = 0.00 Izy = 0.00 Izz = 0.00